the plant journal

SEB Society for Experimental Biology

The Plant Journal (2019) **99,** 815–831 doi: 10.1111/tpj.14423

Chloride as a macronutrient increases water-use efficiency by anatomically driven reduced stomatal conductance and increased mesophyll diffusion to CO_2

Juan D. Franco-Navarro[1,†], Miguel A. Rosales[1,†], Paloma Cubero-Font[1,2], Purificación Calvo[3], Rosario Álvarez[4], Antonio Diaz-Espejo[1] and José M. Colmenero-Flores[1]

[1]*Instituto de Recursos Naturales y Agrobiología,CSIC, Avda Reina Mercedes 10, 41012, Sevilla, Spain,*

[2]*Biochimie et Physiologie Moléculaire des Plantes (BPMP), Univ. Montpellier, CNRS, INRA, SupAgro, 2 Place P. Viala, Montpellier 34060, France,*

[3]*Departamento de Microbiología, Facultad de Biología, Universidad de Sevilla, Avda Reina Mercedes 6,41012, Sevilla, Spain, and*

[4]*Departamento de Biología Vegetal y Ecología, Facultad de Biología, Universidad de Sevilla, Avda. Reina Mercedes 6, 41012, Sevilla, Spain*

Received 21 September 2018; revised 17 May 2019; accepted 22 May 2019; published online 31 May 2019.
*For correspondence (e-mail chemacf@irnase.csic.es).
[†]Both authors contributed equally to this work.

SUMMARY

Chloride (Cl^-) has been recently described as a beneficial macronutrient, playing specific roles in promoting plant growth and water-use efficiency (WUE). However, it is still unclear how Cl^- could be beneficial, especially in comparison with nitrate (NO_3^-), an essential source of nitrogen that shares with Cl^- similar physical and osmotic properties, as well as common transport mechanisms. In tobacco plants, macronutrient levels of Cl^- specifically reduce stomatal conductance (g_s) without a concomitant reduction in the net photosynthesis rate (A_N). As stomata-mediated water loss through transpiration is inherent in the need of C_3 plants to capture CO_2, simultaneous increase in photosynthesis and WUE is of great relevance to achieve a sustainable increase in C_3 crop productivity. Our results showed that Cl^--mediated stimulation of larger leaf cells leads to a reduction in stomatal density, which in turn reduces g_s and water consumption. Conversely, Cl^- improves mesophyll diffusion conductance to CO_2 (g_m) and photosynthetic performance due to a higher surface area of chloroplasts exposed to the intercellular airspace of mesophyll cells, possibly as a consequence of the stimulation of chloroplast biogenesis. A key finding of this study is the simultaneous improvement of A_N and WUE due to macronutrient Cl^- nutrition. This work identifies relevant and specific functions in which Cl^- participates as a beneficial macronutrient for higher plants, uncovering a sustainable approach to improve crop yield.

Keywords: chloride nutrition, beneficial macronutrient, nitrate, water-use efficiency, photosynthesis, stomatal conductance, stomatal density, mesophyll diffusion conductance to CO_2, chloroplast, *Nicotiana tabacum*.

Linked article: This paper is the subject of a Research Highlight article. To view this Research Highlight article visit https://doi.org/10.1111/tpj.14498.

INTRODUCTION

Especially in the agronomic context, chloride (Cl^-) has been traditionally considered a toxic anion rather than a plant nutrient. Due to its abundance and ubiquity in nature, it has been largely believed that Cl^- deficiency is a very rare phenomenon in plants growing in their natural habitats or in agriculture (White and Broadley, 2001). Given the particular precautions that were required by earlier investigators to induce Cl^- deficiency symptoms in different plant species, the relevance of Cl^- in plant growth has been largely neglected (Xu *et al.*, 2000). However, in addition to being an essential micronutrient (Johnson *et al.*, 1957; Xu *et al.*, 2000; White and Broadley, 2001; Marschner, 2011), we have recently shown that, Cl^- is a beneficial macronutrient for plants (Franco-Navarro *et al.*, 2016), a definition further supported by others (Raven, 2017; Wege *et al.*, 2017; Geilfus, 2018).

When supplied to tobacco plants (*Nicotiana tabacum* L.) at concentrations in excess of those needed to satisfy the micronutrient requirements, but insufficient to cause toxicity (1–5 mM Cl^-), Cl^- treatments resulted in leaf accumulation levels that are typical of the content of a macronutrient (Franco-Navarro *et al.*, 2016). Under these conditions, Cl^- has played specific roles in regulating leaf osmotic potential and turgor. Besides improving leaf water balance parameters, Cl^- also alters water relations at the whole-plant level through reduction in plant transpiration. This was a consequence of the reduction in stomatal conductance (g_s), which resulted in lower water loss and greater WUE, measured as intrinsic WUE (WUEi; the ratio of net photosynthesis rate to stomatal conductance) and integrated WUE (long-term ratio of plant biomass production to total water consumed).

Plant WUE has become a key measure of the efficiency of the use of water resources and a target for crop selection and breeding (Linderson *et al.*, 2012; Gago *et al.*, 2014; Tomas *et al.*, 2014). As stomata-mediated water loss through transpiration is inherent in the need for C_3 plants to capture CO_2, there is an urgent need for simultaneously increasing photosynthesis/yield and WUE in C_3 crops (Morison *et al.*, 2008; Flexas *et al.*, 2016). Improved photosynthetic efficiency has played only a minor role in the remarkable increases in agricultural productivity achieved in the last half century. Therefore, it is expected that further increases in crop yield potential will rely in a large part on improved photosynthesis (Long *et al.*, 2006; Zhu *et al.*, 2010; Ort *et al.*, 2015). Modern agriculture requires that the increase in productivity be made in a sustainable way, minimizing the raise of cultivated area and maximizing the efficiency in the use of resources like fertilizers and, especially, water (Gilbert, 2012; Ort *et al.*, 2015; Flexas *et al.*, 2016). Given the effect of Cl^- nutrition on WUE regulation (Franco-Navarro *et al.*, 2016), Cl^- fertilization arises as a potential strategy to manipulate whole WUE in crops, as previously proposed for other agronomic (Gregory, 2004) and biotechnological approaches (Boyer, 1996; Parry *et al.*, 2005; Flexas, 2016; Flexas *et al.*, 2016).

Despite reducing water consumption, the presence of Cl^- has led to a moderate increase in plant fresh and dry biomass, a phenomenon that occurred in parallel with an increase in leaf cell size (including epidermal, mesophyll and stomatal cells) and shoot expansion (Franco-Navarro *et al.*, 2016). Reduction in g_s is expected to reduce atmospheric CO_2 capture, resulting in concomitant reduction in the net photosynthesis rate (A_N). Unexpectedly, the Cl^- treatment did not result in a reduction in A_N when compared with control tobacco plants treated with equivalent amounts of phosphate + sulphate salts (Franco-Navarro *et al.*, 2016). This apparent inconsistency could be explained if the Cl^- treatment also improved the overall carboxylation rate of ribulose-1,5-bisphosphate (RuBP) as a result of: (i) higher ribulose-1,5-bisphosphate carboxylase/oxygenase (RuBisCo) activity; and (ii) higher diffusion rate of atmospheric CO_2 into leaf mesophyll cells and chloroplasts. In the past, it was believed that virtually all the resistance to CO_2 diffusion was caused by stomata. However, it is now clear that the mesophyll diffusion conductance to CO_2 from substomatal cavities to the sites of carboxylation (g_m) accounts actually for more than 40% of the decrease in CO_2 (Flexas *et al.*, 2008; Warren, 2008; Galmés *et al.*, 2013). Therefore, g_m is of great relevance for A_N in many species (Flexas *et al.*, 2012; Muir *et al.*, 2014), also affecting WUE (Flexas *et al.*, 2016). As CO_2 diffuses into the leaf, it must pass through several anatomical and cell barriers: the boundary layer, the stomatal pore, the air-filled pore space within the leaf, the cell wall, the plasma membrane and cytoplasm as well as the chloroplast membrane. Alterations in anatomical and cell parameters such as leaf thickness, cell packing, shape and wall thickness and chloroplasts arrangement to intercellular airspaces can influence the conductance to CO_2 at each step of this diffusion pathway (Terashima *et al.*, 2011; Tosens *et al.*, 2012; Tomas *et al.*, 2013). Leaf anatomical variations induced by macronutrient levels of Cl^- in tobacco leaves, including higher leaf thickness and bigger mesophyll cells could potentially affect g_m (Franco-Navarro *et al.*, 2016). This possibility adds further complexity to attempts to understand the mechanism of genotypic and phenotypic variability of g_m (Raven, 2017).

Positive effects on cell size, biomass increase, osmotic regulation and WUE were specific for Cl^- relative to other mineral macronutrient anions (Franco-Navarro *et al.*, 2016). But it is still unclear how Cl^- could be beneficial, especially in comparison with nitrate (NO_3^-), which in addition to being an essential source of nitrogen, shares with Cl^- similar physical and osmotic properties, as well as common transport mechanisms (Flowers, 1988; Cubero-Font *et al.*, 2016; Li *et al.*, 2017; Wege *et al.*, 2017). Therefore, in this study, we aimed: (i) to confirm whether macronutrient levels of Cl^- in plants reduces g_s without a concomitant reduction in A_N; (ii) to identify physiological/anatomical mechanisms responsible for the observed Cl^--dependent g_s reduction; (iii) to verify whether Cl^- nutrition modifies g_m and which physiological/anatomical alterations rely behind this phenomenon. Understanding these phenomena can be of interest in two respects. The ability to manipulate relevant physiological processes in individuals with the same genetic background is a valuable tool to better understand the studied phenomena. Conversely, a simple and inexpensive agronomic practice like Cl^- fertilization could potentially increase WUE without reducing the photosynthetic efficiency. It is therefore important to understand how Cl^- improves plant growth through the coordinated regulation of WUE and photosynthetic performance.

RESULTS

Effect of Cl^- on plant growth, photosynthesis, leaf water balance and WUE

First, we verified that the 5 mM Cl^- treatment (CL) reproduced the previously reported Cl^--specific responses on plant growth, photosynthesis, water balance and WUE (Franco-Navarro *et al.*, 2016). With this aim the effects of the CL treatment on the parameters of interest were compared with those of plants subjected to low Cl^- treatments (SP and N). Leaf Cl^- concentration in CL-treated plants was around 45–50 mg g^{-1} dry weight (DW) (Figure S1a and Table 1), which is typical of the content of a macronutrient. In SP and N plants, Cl^- concentration was about 100 times smaller, although above the critical level of micronutrient deficiency (Franco-Navarro *et al.*, 2016). No deficiency symptoms like wilting, chlorosis or bronzing were observed in SP- and N-treated plants. In fact, NO_3^--supplemented plants exhibited the best performance in terms of dry biomass and leaf area (Figure S1b–d), ruling out the possibility that plants containing low Cl^- (N and SP plants), were experiencing Cl^- deficiency. The fact that N-treated plants showed the highest growth and biomass was expected given the essential role of nitrogen on plant development (Hawkesford *et al.*, 2012). The positive effect of the Cl^- treatment on growth and biomass was confirmed in the plants used in this work since CL plants showed higher DW and leaf growth than SP plants (Figure S1b–d).

The effect of the Cl^- treatment on leaf water parameters was confirmed in the plants used in this work since CL plants showed higher water content (Figure S2a) and higher relative water content (RWC) (Figure S2b). In consequence, leaves of CL plants were more succulent (Figure S2c) and thicker (Figure S2d). As previously reported (Franco-Navarro *et al.*, 2016) CL plants exhibited more negative osmotic potential than SP and N plants (Figure S2e) and higher turgor potential (Figure S2f).

Compared with N and SP treatments, CL plants showed around 33% reduction in g_s (Figure 1a), producing a concomitant reduction on leaf transpiration as indicated by the Fresh Weight loss assay (Figure 1b). Accordingly, CL plants consumed less water throughout the experiment (Figure 1c). Interestingly, despite the lower g_s, A_N of CL plants was not impaired in comparison with SP plants (Figure 1d), determining a 27% higher WUEi (Figure 1e). Consistent with the lower water consumption, the integrated WUE of CL plants was 25% higher than that of SP and N plants (Figure 1f). No significant differences among treatments were found in other photosynthetic parameters like the maximum rate of RuBP carboxylation (V_{cmax}) and the maximum rate of electron transport (J_{max}). Altogether, the results confirmed the beneficial effect of macronutrient Cl^- nutrition on tobacco plant growth, water balance and whole-plant–water relationships.

Effect of Cl^- on stomatal aperture, stomatal density and stomatal index

To identify which physiological mechanism is responsible for the observed Cl^--dependent g_s reduction, different functional and anatomical parameters influencing stomatal-dependent gas-exchange capacity were studied. The opening ratio, pore size, stomatal density and index values were quantified in plants subjected to CL, SP and N treatments.

After 3 h illumination, CL and SP plants presented the same stomatal aperture ratio (width/length), around 0.24, whereas N plants had 22.5% higher aperture ratio (Figure 2b), around 0.31. These values are within the expected range of fully open stomata (0.18–0.35), previously reported by Willmer and Fricker (1996). During the following 4 h, light-incubated peelings exhibited a progressive stomatal closure, in line with the natural circadian closure occurring in our plants between 15:00 and 19:00 h (Figure 2a). Addition of ABA to the peelings incubation medium determined that plants did not respond to the light treatment (Figure 2c), remaining the stomata as closed as those from non-illuminated control peelings (Figure 2b), with aperture ratio values around 0.045, within the expected range of fully closed stomata (below 0.05) reported by Willmer and Fricker (1996). Interestingly, N plants remained partially open under the ABA treatment,

Table 1 Ion concentration and total nitrogen content in leaves of plants subjected to different treatments

	Ion concentration (mg g^{-1} DW)							
Treatment	K^+	Ca^{2+}	Mg^{2+}	Cl^-	NO_3^-	PO_4^{3-}	SO_4^{2-}	TNC
SP	49.61 ± 3.27	28.10 ± 5.87	8.89 ± 2.08	0.54 ± 0.07 b	8.78 ± 1.29 b	14.28 ± 1.10 a	34.21 ± 4.06 a	63.07 ± 6.66 b
N	50.43 ± 3.27	24.42 ± 3.20	8.11 ± 1.31	0.60 ± 0.08 b	51.03 ± 7.57 a	11.01 ± 1.23 b	19.21 ± 4.15 ab	212.69 ± 19.79 a
CL	49.54 ± 1.88	25.26 ± 4.82	8.15 ± 1.47	52.98 ± 3.40 a	2.59 ± 0.49 b	10.52 ± 0.55 b	14.64 ± 2.07 b	48.82 ± 3.11 b
P-value	ns	ns	ns	***	***	*	*	*

Treatment consisted of the basal nutrient solution supplemented with 5 mM chloride (CL), 5 mM nitrate (N) or the sulphate + phosphate (SP) salt mixture containing the same cationic balance as in the CL and N treatments. Total nitrogen content (TNC) was calculated as the sum of NO_3^- plus organic nitrogen content (mg g^{-1} DW). Mean values ± SE, $n = 6$. 'Homogeneous group' statistics was calculated through ANOVA test, where mean values with different letters are significantly different according to Tukey's test at $P \leq 0.05$. Levels of significance: $P \leq 0.05$ (*); $P \leq 0.001$ (***); and $P > 0.05$ ('ns', no significant differences).

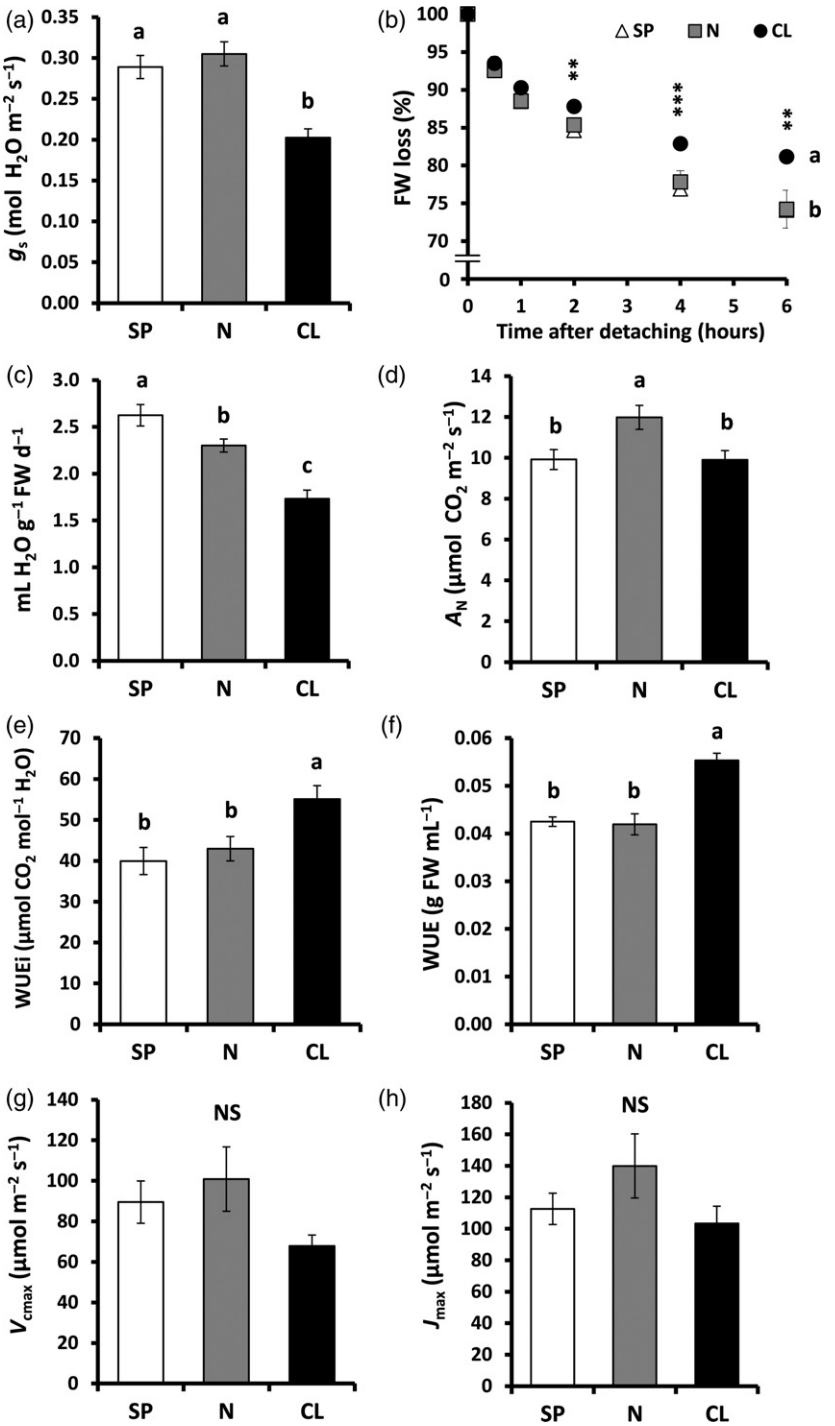

Figure 1. Effect of Cl^- nutrition on gas-exchange parameters and water-use efficiency. Plants were alternatively treated with the following salt supplements: 5 mM chloride salts (CL); 5 mM nitrate salts (N); and a mixture of sulphate + phosphate salts (SP) containing the same cationic balance as in the CL and N treatments. (a) Effect on stomatal conductance (g_s). (b) Effect on leaf transpiration measured as the fresh weight loss (FW loss) of detached leaves over time. (c) Effect on total water consumed throughout the experiment relative to the final fresh biomass (FW). (d) Effect on net photosynthesis rate (A_N). (e) Effect on intrinsic water-use efficiency (WUEi). (f) Effect on integrated water-use efficiency (WUE). (g) Effect on maximum rate of carboxylation (V_{cmax}). (h) Effect on maximum rate of electron transport (J_{max}). Mean values ± SE, $n = 6$. 'Homogeneous group' statistics were calculated through ANOVA (a, c–f) AND MANOVA (b), where mean values with different letters are significantly different according to Tukey's test at $P \leq 0.05$. Levels of significance: $^{**}P \leq 0.01$ and $^{***}P \leq 0.001$.

with aperture ratios around 0.075, 40% higher than those of ABA-treated SP and CL plants (Figure 2c). In addition, when the aperture ratios were compared with those of untreated plants (grown in basal nutrient solution, BS), we observed that all nutritional treatments (SP, N and CL) were able to stimulate stomatal aperture (Figure S3).

We also quantified the absolute stomatal aperture through the measurement of the stomatal pore area and we observed that N and CL plants showed similar pore area values, around 45 μm^2, whereas SP plants showed around 39% less aperture area, corresponding to 27.5 μm^2 (Figure 2d). In summary, results showed that: (i) the N treatment induced the highest aperture ratio; (ii) SP and CL treatments induced lower and similar aperture ratios; and (iii) N and CL treatments exhibited similar stomatal pore areas. The smaller aperture ratio to compensate for larger

pore surface in CL plants is consistent with the higher stomata size in Cl^--treated plants. Therefore, we ruled out the possibility that the lower g_s of CL plants (compared with SP and N plants) were the consequence of a reduced stomatal opening capacity.

These results are consistent with the observation that Cl^- specifically increases the size of different leaf cell types including epidermal, guard, mesophyll and trichome cells (Franco-Navarro *et al.*, 2016). This may alter the distribution of the stomata on the leaf surface. Therefore, Cl^--mediated reduction in g_s can be a consequence of a lower stomatal density (number of stomata per unit area) or a lower stomatal index (percentage of stomata out of the total number of epidermal cells plus stomata). To determine possible alterations in stomatal density and/or stomatal index in CL plants, these parameters were quantified in these cell types (Figure 3). We first confirmed the occurrence of larger epidermal (Figure 3a) and guard (Figure 3b) cells in CL plants. As a direct consequence of the higher cell size, we could verify that epidermal and stomatal density of CL plants were significantly lower than those of SP and N plants (Figure 3c,d, respectively), whereas the stomatal index remained the same in all three treatments (Figure 3e), indicating that the CL treatment regulates stomatal cell size, but not stomatal differentiation.

To ascertain if g_s reduction in CL plants (Figure 1a) can be explained by the lower stomatal density, despite the greater pore area (Figure 2d), the theoretical $g_{w,max}$, which computes the interaction of the stomatal size with the

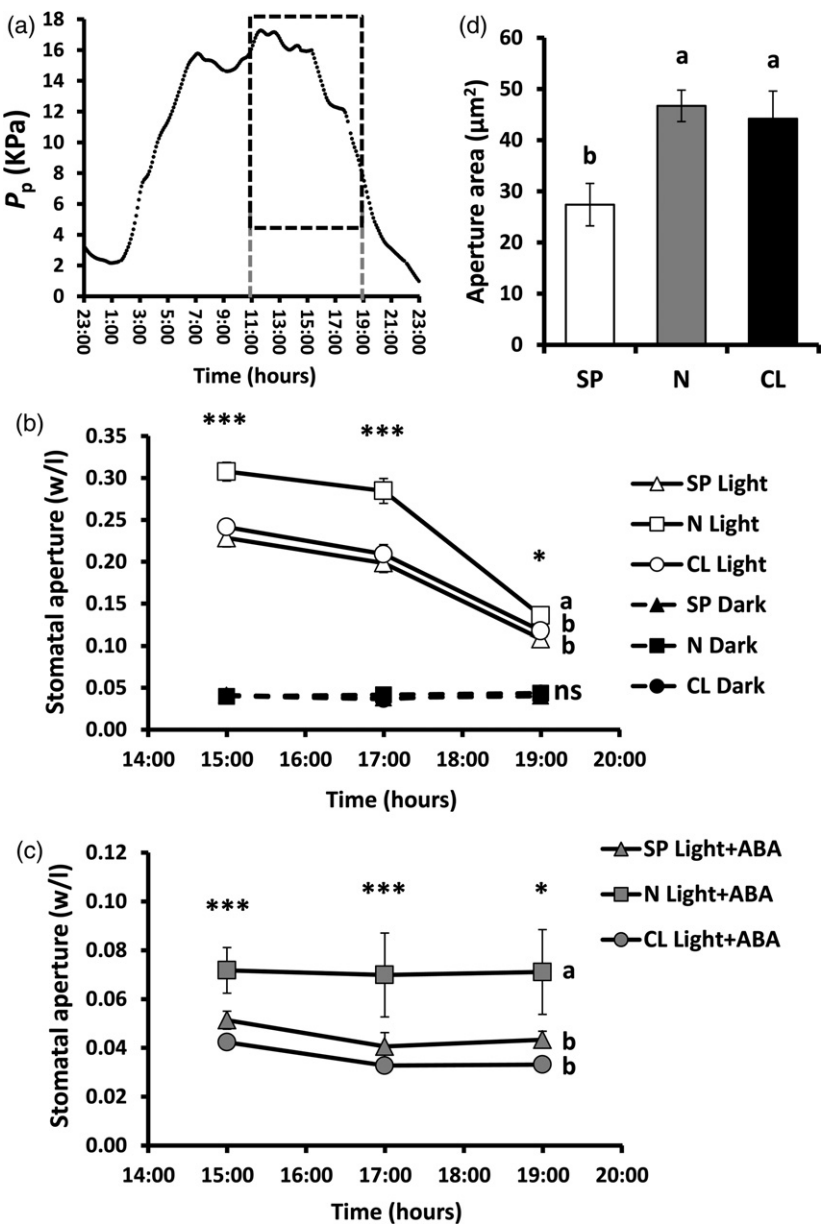

Figure 2. Effect of Cl^- nutrition on stomatal aperture. Plants were alternatively treated with the following salt supplements: 5 mM chloride salts (CL); 5 mM nitrate salts (N); and a mixture of sulphate + phosphate salts (SP) containing the same cationic balance as in the CL and N treatments. (a) Real-time measurement of leaf turgor on a representative plant of the assay using the non-invasive magnetic leaf patch clamp pressure probes (Zimmermann *et al.*, 2008). Patch-pressure (P_p) is inversely correlated with leaf turgor pressure and positively correlated with leaf water potential and plant transpiration (Zimmermann *et al.*, 2008, 2010). P_p values were recorded for 24 h, and the time interval in which the stomatal opening assays were performed, between 11:00 and 19:00 h, is indicated (dotted line box), including the maximal stomata aperture period (lowest leaf turgor between 11:00 and 15:30 h) and the progressive stomatal closure (increasing leaf turgor between 15:30 and 19:00 h). (b, c) Stomatal opening given as the width/length ratio (w/l) quantified from optical microscope images of epidermal peelings obtained at ×40. After synchronizing stomatal closure through a 2 h dark period between, the opening ratios were quantified: in peelings illuminated for 3 h (15:00), 5 h (17:00) and 7 h (19:00) or in control peelings kept in the dark during the same time intervals (b); in peelings treated with 50 μM ABA and illuminated for 3 h (15:00), 5 h (17:00) and 7 h (19:00) (c). (d) Average aperture area (μm^2) of stomata from peelings subjected to 3 h illumination (quantified from the same stomata pictures used for the opening ratio measurements shown in panel (b)). Mean values ± SE are shown. For each time point or treatment and light condition, 30–40 pores were measured. Each experiment was repeated on three separate days using fresh plants (n = 90–120). 'Homogeneous group' statistics were calculated through ANOVA (d) and MANOVA (b, c), where mean values with different letters are significantly different according to Tukey's test at $P \leq 0.05$. Levels of significance: $^*P \leq 0.05$ and $^{***}P \leq 0.001$.

maximum pore area and the stomatal density, was calculated according to the procedure reported by Franks *et al.* (2009). Using the experimentally obtained values of the pore area (Figure 2d), the stomatal cell size (Figure 3b) and the stomatal density (Figure 3d), $g_{w,max}$ was calculated, showing 36.8% lower values for CL plants in comparison with N and SP plants, indicating that a reduction in g_s measured in CL plants was consistent with the reduction in stomatal density.

Effect of Cl^- on mesophyll diffusion conductance to CO_2, mesophyll anatomy and chloroplasts distribution

To uncover the reasons why the specific reduction in of g_s observed in CL plants (Figure 1a) did not result in the expected reduction in A_N (Figure 1d), g_m was estimated. When compared with SP plants, CL plants exhibited significantly higher values of g_m (Figure 4a). N plants presented intermediate values, not significantly different to those of SP and CL treatments. Simultaneous improvement of WUE and A_N in CL plants indicated that Cl^- regulates g_s and g_m independently and, therefore, WUEi should correlate on the ratio g_m/g_s rather than on g_m itself (Flexas *et al.*, 2013). Therefore, Figure 4(b) shows the expected correlation, indicating that Cl^--mediated g_m enhancement was a key factor determining the higher WUE found in this treatment.

To determine which factors were in the origin of the gm enhancement, different anatomical and cellular parameters of the mesophyll were measured. No differences were found in the surface area of mesophyll cells exposed to the intercellular airspaces (Smes; Figure 5a). However, Cl-treated plants showed significantly higher values of Sc and Sc/Smes than SP and N plants (Figure 5b,c), indicating that the CL treatment determined a higher proportion of chloroplasts covering the mesophyll cell surface as a consequence of a higher surface area of chloroplasts exposed to the intercellular airspace of mesophyll cells

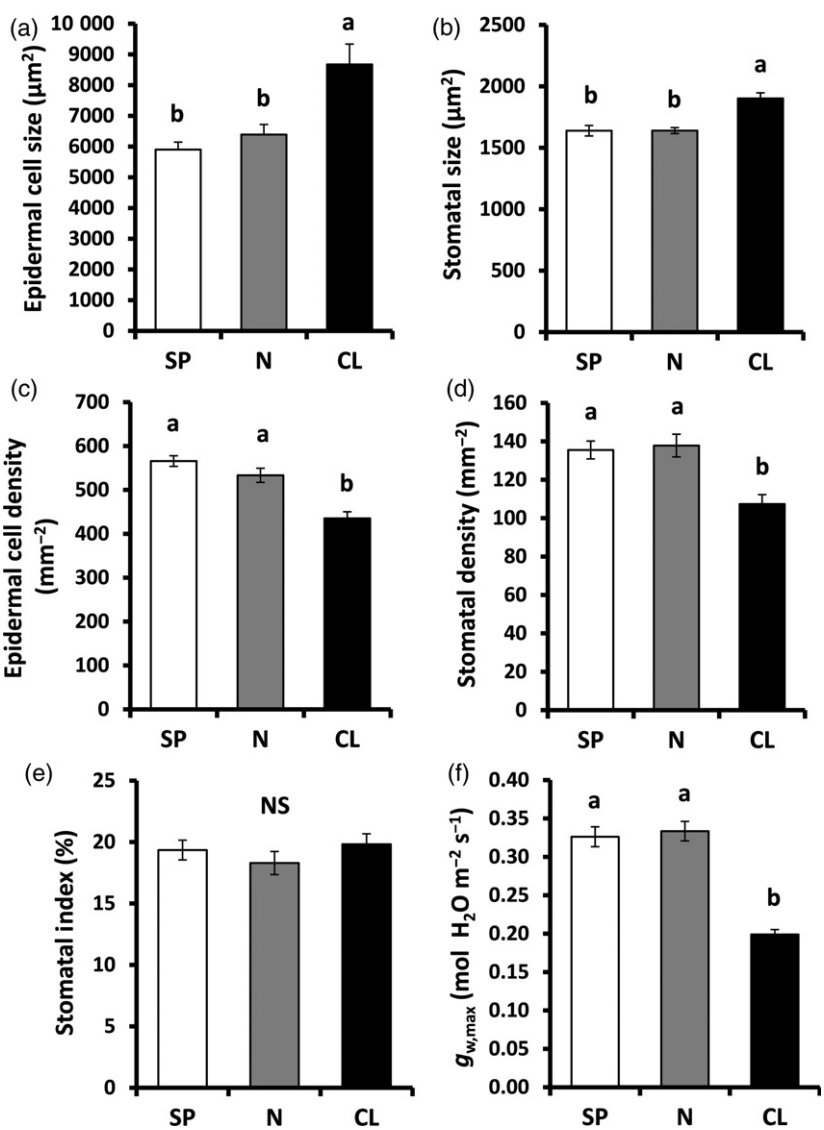

Figure 3. Effect of Cl^- nutrition on epidermal leaf cells size and density. Plants were alternatively treated with the following salt supplements: 5 mM chloride salts (CL); 5 mM nitrate salts (N); and a mixture of sulphate + phosphate salts (SP) containing the same cationic balance as in the CL and N treatments. (a) Effect on epidermal cell size. (b) Effect on stomatal cell size determined by measuring 60 random stomata per treatment. (c) Effect on epidermal cell density. (d) Effect on stomatal cell density. (e) Effect on stomatal index. (f) Modelling of the maximum stomatal conductance according to Franks *et al.* (2009). Mean values ± SE, $n = 6$. 'Homogeneous group' statistics were calculated through ANOVA (a–f), where mean values with different letters are significantly different according to Tukey's test at $P \leq 0.05$. NS, not significant.

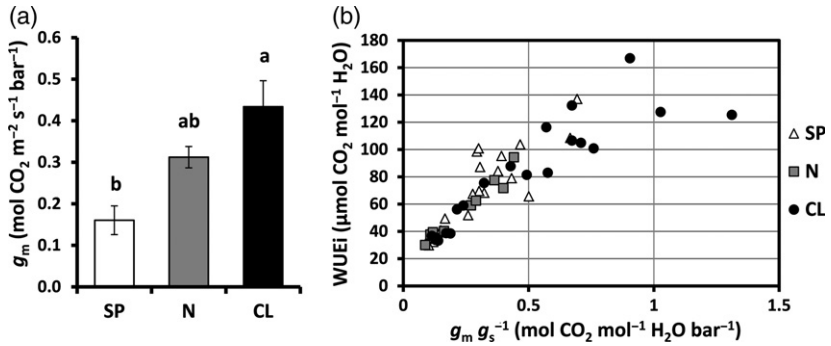

Figure 4. Effect of Cl^- nutrition on mesophyll diffusion conductance to CO_2. Plants were alternatively treated with the following nutritional supplements: 5 mM chloride salts (CL); 5 mM nitrate salts (N); and a mixture of sulphate + phosphate salts (SP) containing the same cationic balance as in the CL and N treatments. Fully expanded photosynthetically active leaves from tobacco plants were used. (a) Effect of nutritional treatments on mesophyll diffusion conductance to CO_2 (g_m). g_m was estimated from simultaneous measurements of leaf gas exchange and fluorescence following the method by Harley *et al.* (1992). (b) Relationship between intrinsic water-use efficiency (A_N/g_s; WUEi) and g_m/g_s. Mean values ± SE, n = 5. 'Homogeneous group' statistics were calculated through ANOVA (a), where mean values with different letters are significantly different according to Tukey's test at $P \leq 0.05$.

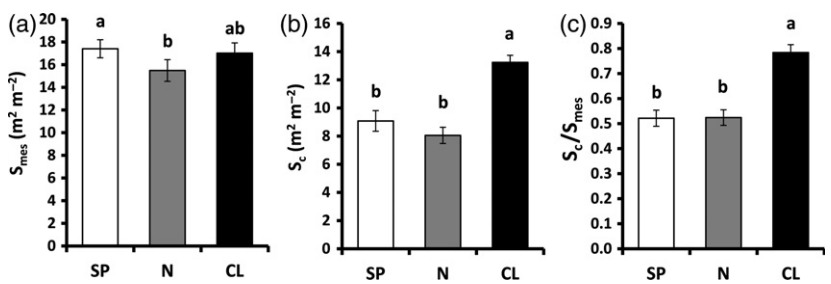

Figure 5. Effect of Cl^- nutrition on mesophyll anatomical parameters. Plants were alternatively treated with the following nutritional supplements: 5 mM chloride salts (CL); 5 mM nitrate salts (N); and a mixture of sulphate + phosphate salts (SP) containing the same cationic balance as in the CL and N treatments. (a) Surface area of mesophyll cells exposed to the intercellular airspaces per unit leaf area (S_{mes}). (b) Surface area of chloroplasts exposed to the intercellular airspace per unit leaf area (S_c). (c) Proportion of chloroplasts covering the mesophyll cell surface (S_c/S_{mes}). Mean values ± SE, n = 10–12. 'Homogeneous group' statistics were calculated through ANOVA (a–c), where mean values with different letters are significantly different according to Tukey's test at $P \leq 0.05$.

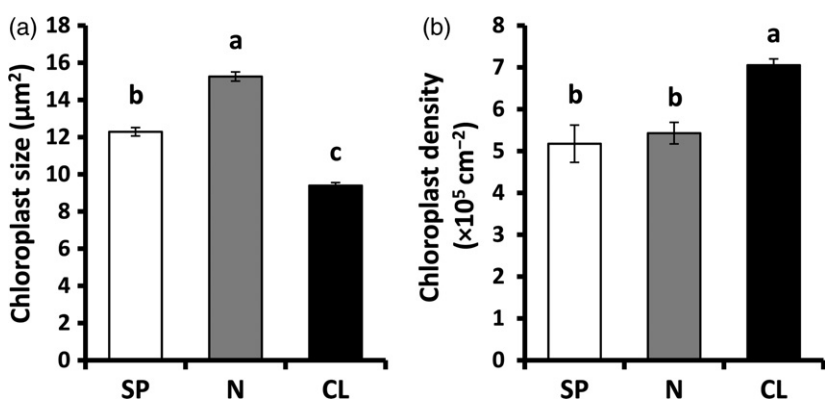

Figure 6. Effect of Cl^- nutrition on the number and size of chloroplasts. Plants were alternatively treated with the following salt supplements: 5 mM chloride salts (CL); 5 mM nitrate salts (N); and a mixture of sulphate + phosphate salts (SP) containing the same cationic balance as in the CL and N treatments. (a) Chloroplast size. (b) Chloroplast density. Mean values ± SE, n = 500 chloroplasts analysed in five plants per treatment. 'Homogeneous group' statistics were calculated through ANOVA (a, b), where mean values with different letters are significantly different according to Tukey's test at $P \leq 0.05$.

Quantification of the size and number of chloroplasts showed that mesophyll cells of CL plants contain a higher number of smaller chloroplasts (Figure 6a,b). Photomicrographs of leaf sections also revealed the occurrence in CL plants of chloroplasts containing bigger starch granules in lacunar and palisade parenchyma cells (Figure S4). Furthermore, measurement of starch content in tobacco leaves confirmed higher content in CL plants in comparison to SP and N plants (Figure 7).

To determine for each treatment which components among the diffusional and biochemical parameters played a major role in modifying A_N, individual contributions

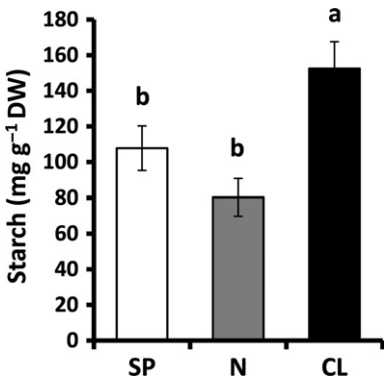

Figure 7. Effect of Cl^- nutrition on leaf starch content.Plants were alternatively treated with the following nutritional supplements: 5 mM chloride salts (CL); 5 mM nitrate salts (N); and a mixture of sulphate + phosphate salts (SP) containing the same cationic balance as in the CL and N treatments. Mean values ± SE, $n = 5$. 'Homogeneous group' statistic was calculated through ANOVA, where mean values with different letters are significantly different according to Tukey's test at $P \leq 0.05$.

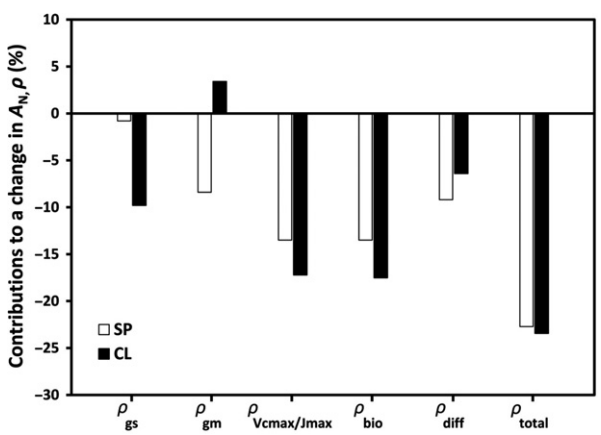

Figure 8. Relative limitations on A_N. Contributions (ρ) of individual variables (g_s, stomatal conductance; g_m, mesophyll diffusion conductance to CO_2; and $V_{c,max}$, maximum velocity of carboxylation or J_{max}, maximum rate of electron transport) to the reduction in net photosynthesis rate (A_N) shown by CL and SP plants using the values of N plants as reference. $\rho_{Vcmax/Jmax}$ does not represent the contribution of the ratio V_{cmax}/J_{max} but the contribution of each value.

directly related to CO_2 uptake and fixation were calculated according to Buckley and Diaz-Espejo (2015). With this aim, the g_s, g_m, and $V_{c,max}/J_{max}$ contributions were quantified in CL and SP plants using as reference the values of N plants (the treatment with the highest photosynthetic rate; Figure 8). Regarding the diffusional components, the higher limitation imposed by g_s reduction in CL plants (−9.0% compared to SP plants) was compensated by a lower g_m limitation (+13.2% in CL plants compared with SP plants), resulting in total diffusional limitations (ρ_{diff}) of −6.4% for CL plants and −9.2% for SP plants. The biochemical components ($\rho_{Vcmax/Jmax}$) determined a greater limitation for CL plants (−17.2%) than for SP plants (−13.5%), probably as a consequence of the lower leaf nitrogen content of CL plants (Table 1). Therefore, total photosynthetic limitation (ρ_{total}) of CL plants (−23.4%) was very similar to that of SP plants (−22.7%), in agreement to the similar A_N values experimentally obtained for both treatments (Figure 1d). Altogether, these results showed that Cl^- improves CO_2 conductance in the mesophyll, which compensates for the limitation produced by the reduction in stomatal conductance.

DISCUSSION

We demonstrated that Cl^- supplementation in the range 1–5 mM increased DW, WUE, cell size and leaf growth in tobacco plants (Franco-Navarro *et al.*, 2016). This work attempts to reveal what is the specific beneficial role of Cl^- on plant growth and development when it is provided to macronutrient levels, and how it can be reconciled with the g_s reduction observed in these plants. We first verified that the previously reported effects of Cl^- on the growth and water relations of tobacco plants (Franco-Navarro *et al.*, 2016) were clearly reproduced in the plants used in this study. The 5 mM Cl^- treatment resulted in: (i) higher dry biomass and greater leaf area (Figure S1); (ii) improved leaf water balance parameters, including Water Content (WC), RWC, succulence, leaf thickness, tissue osmolarity and turgor (Figure S2); and (iii) greater WUE as a consequence of a lower g_s that reduced leaf transpiration and increased both photosynthetic and intrinsic WUE (Figure 1). This work elucidates: the physiological mechanism responsible for the observed Cl^--dependent g_s reduction; how this phenomenon can be, in turn, compatible with the stimulation of higher growth in tobacco plants; and the physiological and cellular basis behind the beneficial effect of Cl^- on plant growth when this element accumulates to levels that are typical of the content of a macronutrient.

Effect of nutritional treatments on stomatal opening

Stomatal opening is a crucial mechanism in the regulation of gas exchange. It has been proposed that rather than anatomical alterations, changes of stomatal opening is the most important factor regulating g_s and WUEi (Paoleti and Gellini, 1993). In fact, the role of anion transporters on the regulation of stomatal closure is a well known phenomenon at the cellular and molecular level. Particularly, anion channels such as SLAC1 and SLAH3, which mediate Cl^- and NO_3^- release from guard cells, are the components that connect the ABA-mediated signalling of environmental cues with the physical events that trigger stomatal closure (Negi *et al.*, 2008; Vahisalu *et al.*, 2008; Meyer *et al.*, 2010; Geiger *et al.*, 2011). High content of Cl^- in leaf tissues of CL plants, for example, concentrations ranging 100–150 mM Cl^- (Franco-Navarro *et al.*, 2016), might alter

the flow of anions from epidermal cells, for example due to high extracellular accumulation of the anion, therefore modifying regulatory properties of stomatal activity. However, we proved that the Cl^--dependent reduction in g_s did not result from a lower stomatal opening (Figure 2). First, plants supplemented with any of the nutritional treatments SP, N and CL, increased their stomatal opening capacity in comparison with plants grown with the BS (Figure S3). Second, the CL and SP treatments resulted in the same stomatal opening (width to length ratio; Figure 2b,c). Third, the absolute stomatal pore area of CL plants was 39% greater than that of SP plants (Figure 2d). Therefore, we could conclude that Cl^- does not induce a greater stomatal closure.

The nutritional treatments (SP, N and CL) clearly pointed to a role of inorganic ions in the induction in stomatal aperture according to their availability (Figure S4). Mineral nutrition is one of the factors affecting plant growth and water relations (Cramer *et al.*, 2009). The three nutritional supplements have in common the same concentration of cations, including potassium (K^+, 2.5 mM), calcium (Ca^{2+}, 0.6 mM), and magnesium (Mg^{2+}, 0.6 mM). The importance of potassium (K^+) in plant performance and photosynthetic efficiency is a well known phenomenon. The nutritional treatments (SP, N and CL) increased K^+ concentration from 2.1 mM (in the BS solution) to 4.6 mM (Table S1). In *Laurus nobilis*, K^+ application resulted in a 45% increase in the transpiration rate 24 h after fertilization (Oddo *et al.*, 2011). It is not clear, however, which cellular, biochemical or physiological factors are directly involved in this response. Losch *et al.* (1992) concluded a beneficial effect of K^+ supply on WUE as a consequence of altered stomatal sizes and densities. However, in this work K^+ was applied as KCl and the specific effects of Cl^- on the parameters measured were not controlled.

Interestingly, the NO_3^- treatment (N) induced an even greater stomatal opening ratio compared to the other supplements applied (SP and CL; Figure 2b), even in the presence of ABA (Figure 2c). This phenomenon is possibly related to the higher A_N observed in N plants (Figure 1d). Plants treated with an additional supply of 5 mM NO_3^- (N plants), presented higher leaf NO_3^- and total nitrogen content (TNC; Table 1). The bulk of leaf nitrogen is associated with photosynthetic enzymes, particularly ribulose-1,5-bisphosphate carboxylase/oxygenase (RuBisCo), resulting in a strong positive correlation between A_N and leaf TNC (Schulze *et al.*, 1994; Wright *et al.*, 2003), as observed in Figure 1(d), where N plants presented 17% higher A_N than SP and CL plants. It has been proposed that higher leaf TNC increases the availability of photosynthetic protein, which improves the assimilation rate of CO_2 (Cramer *et al.*, 2009). Although N plants showed higher V_{cmax} and J_{max} values (Figure 1g,h), no statistically significant differences with CL and SP plants were observed. It has been in turn been proposed as a positive regulation of g_s by leaf nitrogen content, which has been quantified using both ecological (Schulze *et al.*, 1994) and physiological (Wilkinson *et al.*, 2007) approaches. It is not clear, however, if the proposed nitrogen-dependent g_s regulation relies on the control of the stomatal aperture, the stomatal density, or both. Our results indicate that the increase in leaf TNC observed in N plants leads to a higher stomatal aperture (Figure 2b, c), not affecting the stomatal density (Figure 3d).

Effect of Cl^- nutrition on epidermal cell size and stomatal density

While macronutrient Cl^- nutrition did not induce stomatal closure, it decreased stomatal density (number of stomata per unit area; Figure 3d). Stomatal density is an important eco-physiological parameter that affects gas exchange and photosynthesis (Pompelli *et al.*, 2010). During leaf ontogenesis, stomatal density is firstly determined by stomatal initiation and later by epidermal cell expansion. Therefore, stomatal density is a function of cell size (Salisbury, 1928), which explains that the increase in the size of epidermal cells in CL plants (Figure 3a,b) is in the origin of the reduced stomatal density (Figure 3d). Conversely, the stomata index (percentage of stomata out of the total number of epidermal cells plus stomata), which might imply a biological impact on stomatal development (Ticha, 1982; Lake *et al.*, 2001), is independent of cell size (Salisbury, 1928), and was not affected by the nutritional treatments (Figure 3e). Various environmental factors such as irradiance, water deficit and salinity modify the absolute values of stomatal density and stomatal sizes, without affecting the ontogenic pattern of the changes (Ticha, 1982). Our results showed that rather than the biogenesis of stomata, Cl^- affects the size and the density of different leaf cell types, including that of guard cells (Figure 3).

The larger size of stomata in CL plants is also in agreement with its greater stomatal pore area (39% compared with the SP plants; Figure 2d). Although this may seem contradictory to the decreased g_s, the calculation of the maximum pore area according to Franks *et al.* (2009), showed that the effect of a lower stomatal density in CL plants is more determinant than that of a larger pore size to explain the eventual effect on decreasing g_s (Figure 3f). This $g_{w,max}$ reduction value (36.8%) was similar to the 33.3% reduction in g_s calculated for CL plants (Figure 1a). Therefore we could conclude that the lower stomatal density accounts for the lower g_s quantified in Cl^--treated plants.

Effect of Cl^- nutrition on photosynthetic efficiency

Despite the reductions in both g_s and water consumption, CL plants exhibited similar A_N values than SP plants. This implies the existence of a compensatory factor that allows

CL plants to maintain the same CO_2 assimilation rate despite the lower g_s (Figure 1d). In well grown C_3 plants under light-saturated and ambient CO_2 conditions, this compensatory factor may consist of an increase in the carboxylation capacity of RuBisCo (V_{cmax}; Farquhar *et al.*, 1980) and/or the leaf internal diffusion to CO_2 (g_m; Warren, 2008; Flexas *et al.*, 2008). The possibility that the CL treatment enhanced the carboxylation capacity of RuBisCo was ruled out given that CL plants did not exhibit either higher V_{cmax} or J_{max} values than SP or N plants (Figure 1g,h). Furthermore, calculating the relative limitations of A_N (Figure 8) showed that this biochemical component ($\rho_{Vcmax/Jmax}$) determined a higher limitation in CL plants (−17.2%) in comparison with SP plants (−13.5%), probably as a consequence of the lower leaf TNC of CL plants (Table 1). This ruled out also the possibility of higher content of RuBisCo and electron-transport proteins in CL plants, which together represent more than 50% of leaf TNC as shown in Xiong *et al.* (2017). It is difficult also that in the origin of the mentioned compensatory effect is the role of Cl^- in stabilization of the water splitting system of photosystem II. This mechanism, described to be absolutely Cl^--specific (Marschner, 2011), requires only two Cl^- molecules in each oxygen-evolving complex (Kawakami *et al.*, 2009). This means leaf nutrient concentrations well below the Cl^- deficiency threshold (Terry, 1977) and much lower than that present in SP and N plants (Table 1). Therefore, the N and SP treatments do not compromise the stability of the photosystem II, as evidenced by the fact that N plants have the highest A_N values (Figure 1d), despite having leaf Cl^- concentrations under the macronutrient content of CL plants.

Effect of Cl^- nutrition on mesophyll diffusion conductance to CO_2

A_N is greatly influenced also by the diffusion rate of atmospheric CO_2 into leaf mesophyll cells and chloroplasts. It was believed that virtually all the resistance to CO_2 diffusion was caused by stomata. However, it is now clear that leaf internal diffusion or the mesophyll diffusion conductance to CO_2 from substomatal cavities to the sites of carboxylation (g_m) accounts actually for more than 40% of the decrease in CO_2 (Flexas *et al.*, 2008; Warren, 2008; Galmés *et al.*, 2013). As g_m is a factor independent of g_s, it may simultaneously increase A_N and WUE without concomitantly increasing g_s (Flexas *et al.*, 2013; Tomeo and Rosenthal, 2017). This phenomenon has been observed to occur in Cl^--treated plants, strongly suggesting that, besides reducing g_s, Cl^- nutrition improves g_m. CL leaves showed 60% and 30% more g_m than SP and N, respectively, supporting the role of g_m in the maintenance of A_N despite the decrease in g_s. Leaf structural components such as leaf thickness, size, shape, mesophyll cells packing (porosity), and cell wall width are major factors determining g_m (Hassiotou *et al.*, 2009; Tomas *et al.*, 2013; Muir *et al.*, 2014). Anatomical alterations produced by the CL treatment in the leaf, including greater cells and leaf succulence (Franco-Navarro *et al.*, 2016; Figure S2) may alter CO_2 diffusion to the chloroplast. It has been reported for example that the macronutrient K^+ can modify g_m through anatomical variation of mesophyll conductance. Therefore, K^+ deficiency leads to a reduction in the mesophyll surface area exposed to intercellular airspace per unit leaf area, giving rise to a reduction in g_m (Lu *et al.*, 2016). In plants treated with macronutrient levels of Cl^-, the size of palisade and spongy cells of CL plants is about 1.7 and 2.0 times greater than that of SP and N plants, respectively (Franco-Navarro *et al.*, 2016). It is expected that higher cell size ultimately determines lower surface-to-volume ratio of mesophyll cells and a lower exposition to the intercellular air space (S_{mes}). However, we did not find significant differences among treatments in S_{mes} (Figure 5a). Besides the exposure area of mesophyll cells, g_m is highly dependent on the chloroplast surface area facing the intercellular spaces S_c (Evans *et al.*, 1994; Terashima *et al.*, 2006; Tomas *et al.*, 2013) and chloroplast size (Li *et al.*, 2009). Interestingly, macronutrient Cl^- concentrations were determined to be about 35% higher S_c (Figure 5b), most probably due to the higher density of chloroplasts present in CL plants (Figure 6b). However, these changes in S_c does not appear to be enough to explain either the g_m values obtained from gas exchange coupled with leaf chlorophyll fluorescence as previously described in the literature (Tomas *et al.*, 2013; Carriqui *et al.*, 2019) or to explain the differences among treatments. To explain the discrepancy between both estimations of g_m, it is possible that we had mathematical artefacts (Gu and Sun, 2014) or errors derived from the over-simplification of the model used (Tholen and Zhu, 2011; Xiao and Zhu, 2017). The other possibility is a higher influence of biochemical factors such as aquaporins or carbonic anhydrase. Both molecules are able to modify and regulate CO_2 diffusion inside the leaf (Uehlein *et al.*, 2003; Flexas *et al.*, 2006; Terashima *et al.*, 2011; Momayyezi and Guy, 2017). If that were the case it would imply that there is not a linear correlation between the anatomical parameters that enhance g_m, such as S_c, and the actual g_m value.

However, the most likely factor that compensates for the loss of stomatal conductance in Cl^--treated plants is still the enhancement of g_m (Figure 8), allowing CL plants to maintain a photosynthetic capacity similar to that of SP plants (Figure 1d). Anatomical parameters, although apparently insufficient, varied in the expected direction in the CL plants, and are important to explain the maintenance of A_N.

Effect of Cl^- nutrition on chloroplast density

The question arises why the number of chloroplasts increased in plants treated with Cl^-. A close correlation between the leaf mesophyll cell size and the number of

chloroplasts within the cell indicates that cell size is a primary determinant of the chloroplast number (Dean and Leech, 1982; Pyke and Leech, 1987). Then, the higher chloroplast density in CL plants could be somehow determined by the higher size of spongy and palisade cells of Cl^--treated plants (Franco-Navarro *et al.*, 2016).

Chloroplasts divide by a process of binary fission. After differentiation from proplastids, chloroplasts undergo a set of divisions during mesophyll cell expansion to generate a large population of small chloroplasts (Pyke, 2010). *Arabidopsis thaliana arc* (*accumulation and replication of chloroplast*) mutants impaired in chloroplast division, contain a lower number of larger chloroplasts (Pyke and Leech, 1992). Given that CL plants have a higher number of smaller chloroplasts (Figure 6), our results surprisingly pointed to the involvement of Cl^- in chloroplast division. Adequate chloroplast division is expected to have positive effects on g_m for different reasons. First, a higher surface-to-volume ratio of smaller chloroplasts could increase the efficiency in the exchange of molecules between the chloroplast and the cytosol, favouring the diffusion of CO_2. Second, a higher S_c/S_{mes} is expected to provide more parallel paths for CO_2 diffusion from the intercellular airspace into the chloroplasts, a very important factor promoting higher g_m (Evans and Loreto, 2006; Terashima *et al.*, 2006; Galmés *et al.*, 2013). Therefore, *A. thaliana arc* mutants containing smaller populations of larger chloroplasts show important reductions in g_m and photosynthetic rate (Weise *et al.*, 2015; Xiong *et al.*, 2017). Whereas this phenomenon was clearly associated with a lower S_c, no significant differences were observed between the mutants and their wild-types in V_{cmax} and J_{max} values (Xiong *et al.*, 2017). Similarly, SP and N plants containing smaller populations of larger chloroplasts showed lower values of g_m and S_c, without being affected in their photochemical capacity. Therefore, a clear parallelism between Cl^- deficiency and the phenotype of *arc* mutants has been established that reinforces the proposed participation of Cl^- on chloroplasts division. Furthermore, strong reduction in starch grain reserves has been described as a consequence of the inhibition of chloroplast biogenesis induced by light deprivation during embryo maturation in Arabidopsis (Liu *et al.*, 2017), a fact that correlates with the stimulation of starch content in CL plants (Figures 7 and S4).

The reason why chloride nutrition is involved in chloroplast division remains unknown. The number of chloroplasts per cell is regulated by environmental factors and abiotic stress responses such as CO_2 concentration (Teng *et al.*, 2006) and temperature (Jin *et al.*, 2011). Chloroplast density is reduced by 41% in mesophyll cells of manganese-deficient pecan leaves, while the existing chloroplasts preserved their full photochemical competence (Henriques, 2004). Recent publications have shown that a reduction in RWC at the cellular level is the primary trigger of leaf ABA biosynthesis (McAdam and Brodribb, 2016; Sack *et al.*, 2018), being mesophyll cells the main site of biosynthesis (McAdam and Brodribb, 2018). As plants treated with Cl^- have a better water status, with significantly higher values of RWC (Figure S2b), a lower ABA baseline content could be expected to occur in leaves of CL plants. Given that a long-term ABA treatment induces growth suppression and inhibits chloroplast division in mesophyll cells (Wang *et al.*, 2018), macronutrient Cl^- levels determining higher RWC and lower ABA accumulation could contribute to induce both higher leaf cell expansion and chloroplast biogenesis, leading to higher g_m in CL plants. We are currently exploring this hypothesis.

The chloroplast envelope and the thylakoid membrane exhibit a high permeability for Cl^- (Heber and Heldt, 1981; Bose *et al.*, 2017). At sunrise during illumination, Cl^- influx from the stroma to the lumen is essential for thylakoid swelling. Conversely, Cl^- re-export to the stroma would cause the thylakoid to shrink at sunset (Hind *et al.*, 1974; Bose *et al.*, 2017). Similar to the role played by Cl^- in promoting cell turgidity and cell elongation (Franco-Navarro *et al.*, 2016; Wege *et al.*, 2017), regulation of thylakoid swelling suggests a possible role of Cl^- in regulating adequate chloroplast osmolarity and growth, a prerequisite for its subsequent division (Pyke, 2010). Cl^- fluxes also play important roles in the regulation of photosynthetic electron transport and photoprotective mechanisms in chloroplasts. The accumulation of protons in the thylakoid lumen is electrically counterbalanced by Cl^- influx (Enz *et al.*, 1993; Bose *et al.*, 2017), indicating that Cl^- regulates the generation of the pH gradient between the lumen and stroma (Geilfus, 2018). Adequate Cl^- homeostasis, regulated by the thylakoid anion channels AtCLCe, AtVCCN1, and AtVCCN2, is required to adjust photosynthesis to fluctuating light and environmental conditions (Kirchhoff, 2014; Duan *et al.*, 2016; Herdean *et al.*, 2016a, 2016b; Szabo and Spetea, 2017). Therefore Cl^- is important for the proper functioning of the chloroplast in thylakoid swelling regulation and in the progress of the photosynthetic activity, introducing an element of specificity (e.g. it requires Cl^--specific channels) that, at least in part, may explain the requirement of Cl^- over similar molecules such as NO_3^-.

In conclusion, this work identifies relevant and specific functions in which Cl^- participates as a beneficial macronutrient for higher plants. Here, Cl^- stimulates larger leaf cells resulting in a reduction in stomatal density, which in turn reduces g_s and water consumption improving RWC and plant water relations. Conversely, Cl^- improves g_m and photosynthetic performance due, at least in part, to the stimulation of a higher density of smaller chloroplasts that gives rise to both a higher proportion of chloroplasts (with higher surface-to-volume ratio) covering the mesophyll cell surface. The increase in g_m simultaneously with the reduction in g_s, allow Cl^--treated plants to improve

their WUE, which could be of great relevance to improve the productivity of C_3 crops.

EXPERIMENTAL PROCEDURES

Plant cultivation and experimental design

Tobacco plants (*Nicotiana tabacum* L. var. Habana) were grown under greenhouse conditions at 25 ± 3°C/17 ± 2°C (day/night), a relative humidity of 60 ± 10% (EL-1-USB Data-logger; Lascar Electronics Inc., Erie, PA, USA, https://www.lascarelectronics.com/), a 16 h/8 h photoperiod with a photosynthetic photon-flux density (average PAR) of 300–350 μmol m^{-2} sec^{-1} (quantum sensor, LI-6400; Li-COR, Lincoln, NE, USA, https://www.licor.com/) and a luminous emittance of 9000–10 000 lx (Digital Lux Meter, LX1010B; Carson Electronics, Valemount, Canada, http://www.carsons.ca/). Tobacco seeds were sown in flat trays (cell size 4 cm × 4 cm × 10 cm) containing peat that had been previously washed with the corresponding nutrient solution. After 2 days vernalisation in a cold chamber (4°C), seedbeds were transferred to the greenhouse. Three weeks later (21 days after sowing, DAS), seedlings were transplanted to 7.5 L pots (pot size 20 cm × 17 cm × 25 cm), containing a mix of perlite:vermiculite (4:6), where plants were watered with different nutrient solutions described below.

In Johnson *et al.* (1957), 50 μM Cl^- was established as the treatment ensuring Cl^- micronutrient requirements in different plant species, whereas deficiency symptoms were obtained in plants with no Cl^- addition. In this work, 75 μM Cl^- (added as 11 μM $CoCl_2$ and 53 μM KCl) was chosen to be always present in the basal nutrient solution (BS) to fulfil plant Cl^- requirements as a micronutrient in low Cl^- treatments. Other nutrients present in the BS solution were: 1.25 mM KNO_3, 0.725 mM KH_2PO_4, 0.073 mM K_2HPO_4, 2 mM $Ca(NO_3)_2$, 1 mM $MgSO_4$, 0.1 mM FeNa-EDTA, 0.1 mM H_3BO_3, 0.1 mM $MnSO_4$, 29 μM $ZnSO_4$; 0.1 μM $CuSO_4$, 1 μM Na_2MoO_4, and 5 μM KI.

Treatments were performed with the application of 5 mM Cl^- (CL treatment), which included the following salt mixtures supplemented to the BS solution: 2.5 mM KCl, 0.625 mM $MgCl_2$, and 0.625 mM $CaCl_2$. To evaluate the specificity of Cl^- in the studied phenomena, two additional treatments were used: the nitrate (NO_3^-) treatment (N) supplement containing 2.5 mM KNO_3, 0.625 mM $Mg(NO_3)_2$, and 0.625 mM $Ca(NO_3)_2$; and the sulphate + phosphate (SO_4^{2-} + PO_4^{3-}) treatment (SP) supplement containing 1.25 mM KH_2PO_4, 0.625 mM K_2SO_4, 0.625 mM $MgSO_4$, and 0.625 mM $CaSO_4$. The three treatments (CL, N and SP) contained the same cationic balance as shown in the resulting concentration of ions given in Table S1. All experimental solutions were adjusted to pH 5.7 with KOH.

Pots were irrigated up to field capacity (3.5 mL g^{-1} substrate) throughout the experiment. Gas-exchange measurements were performed from 56 to 62 DAS, always around 12 pm. For stomatal aperture assays, leaf-peeling samples were obtained between 11 am and 13 pm. Leaf samples for tissue water balance and plant water relations, for histological sections (anatomy) and for starch quantification were obtained before sunrise (predawn). Especial care was taken to sample subsequently each treatment to avoid any time effect on the values. After 7 weeks (72 DAS), shoots were harvested and leaf area was measured as explained later. Fresh weight (FW) values were obtained, and samples were dried in a forced-air oven at 75°C for 48 h to obtain the DW.

Nutrient content determination

For the determination of nutrient content, fully photosynthetic and expanded mature leaves (non-senescent) were used. Oven-dried leaf tissue was ground to powder using a homogenizer (Taurus, 25790 Barcelona, Spain, https://taurus-home.com/en) and the concentration of Cl^-, NO_3^-, SO_4^{2-}, PO_4^{3-}, and cations was determined as previously reported (Franco-Navarro *et al.*, 2016). Total nitrogen (N) content (TNC) was calculated as the sum of NO_3^- plus organic N content (mg g^{-1} DW), according to the methodology previously reported (Rios *et al.*, 2010).

Water parameters

WC, RWC, succulence, leaf osmotic potential (Ψ_π) and leaf transpiration of individual detached leaves (performed through the FW loss assay) were determined as described before (Franco-Navarro *et al.*, 2016). Integrated WUE was calculated as the final FW obtained after harvesting related to total water consumption (g FW mL^{-1} H_2O) (Abbate *et al.*, 2004).

Stomatal aperture

In order to determine the optimal period of time to set the stomatal aperture assays, *in-planta* natural stomatal opening and closure was determined through real-time leaf turgor recording using non-invasive leaf patch-clamp pressure probes (LPCP) according to the methodology previously described (Zimmermann *et al.*, 2008). Stomatal aperture assays were performed with peelings of abaxial leaf epidermis, according to Allen *et al.* (1999) and He *et al.* (2013), with slight modifications. Peels were obtained from the abaxial surface by gently ripping the epidermis with a scalpel and removing it with tweezers. According to LPCP results (Figure 2a), treatments were performed during the time interval (11:00–19:00 h) that includes both the maximal P_p value (minimal leaf turgor at 11:00–15:30 h) and the progressive turgor recovery (at 15:30–19:00 h), according to the intrinsic plants circadian-rhythm of stomata opening and closure that also operates in epidermal strips (Meidner and Willmer, 1993). Peels were transferred to the incubation buffer (10 mM MES-KOH pH 6.5, 10 mM KCl and 50 μM $CaCl_2$) under dark condition over 2 h (11:00–13:00 h) to induce stomatal closure. Then, peelings were alternatively transferred to light conditions, to light conditions supplemented with 50 μM abscisic acid (ABA), or kept in darkness. A commonly accepted way to measure stomatal aperture is to report the pore width to length ratio (Meidner and Willmer, 1993). Examination of stomatal pore was performed on a Zeiss Axioskop microscope equipped with Nomarski optics, AxioCam MRc5, and the Zeiss AxioVision software (Freeware 'Carl Zeiss AxioVision Rel.4.9.1.0' available in Zeiss Homepage, Carl Zeiss Microscopy GmbH, Jena, Germany, http://www.zeiss.com/). To quantify the pore opening area in μm^2, the outline tool of the AxioVision Software was used.

Photosynthesis, leaf gas exchange and mesophyll diffusion conductance to CO_2

Leaf gas-exchange measurements were conducted between 12:00 and 14:00 h using an open gas-exchange system (LI-6400; LI-COR) equipped with 2 × 3 cm LED chamber (LI-6400-02B). For each treatment, three photosynthetically active and fully expanded intermediate leaves from six plants (52–62 DAS) were used. Photosynthesis was induced with ambient light and 400 μmol mol^{-1} CO_2 surrounding the leaf (C_a). Cuvette conditions were maintained at a photosynthetic photon-flux density (PPFD) of 1600 μmol m^{-2} sec^{-1} (provided by the light source of the Li-6400 with 10% blue light), leaf temperature was maintained at 25°C, flow rate was set at 300 μmol sec^{-1} and the leaf-to-air vapour pressure deficit was kept between 1 and 1.3 kPa. A minimum time between 2 and 3 min was waited for equilibrium before measurements were recorded. These conditions were kept constant for the determinations of net photosynthetic rate (A_N;

μmol CO_2 m^{-2} sec^{-1}) and stomatal conductance (g_s; mol H_2O m^{-2} sec^{-1}). The intrinsic water-use efficiency (WUEi) was calculated as the ratio between photosynthesis rate and stomatal conductance (A_N/g_s; μmol CO_2 mol^{-1} H_2O).

Mesophyll diffusion conductance to CO_2 (g_m) was estimated by two methods: (i) simultaneous measurements of leaf gas exchange and chlorophyll fluorescence (Harley *et al.*, 1992) using the open gas-exchange system equipped with an integrated fluorescence chamber head (LI-6400-40, LI-COR, Lincoln, NE, USA, https://www.licor.com/), and (ii) the curve fitting method (Ethier and Livingston, 2004). A preliminary test was carried out to compare both methods. This test was performed in 12 different leaves including leaves of all three treatments. No significant differences were found between both methods (Figure S5) and the agreement was good.

To estimate g_m from combined gas-exchange and chlorophyll a fluorescence measurements, the actual photochemical efficiency of photosystem II (ϕPSII) was determined by measuring steady-state fluorescence (F_s) and maximum fluorescence during a light-saturating pulse of ca. 8000 μmol m^{-2} sec^{-1} ($F_{m'}$) following the procedures of Genty *et al.* (1989):

$$\phi\mathrm{PSII} = (F_{m'} - F_s)/F_{m'}$$

The electron transport rate (J) was then calculated as:

$$J = \phi\mathrm{PSII} \cdot \mathrm{PPFD} \cdot \alpha \cdot 0.5$$

where PPFD is the photosynthetic photon-flux density and α represents the leaf absorptance and 0.5 the partitioning of absorbed quanta between photosystems I and II. α was previously determined using an integrating sphere and a field-portable spectroradiometer (Li-1800; LI-COR, Lincoln, NE, USA, https://www.licor.com/)) to measure reflectance and transmittance of leaf tissue samples inside a dark chamber at 2-nm intervals between 465 nm (blue light) and 670 nm (red light), as described in Schultz (1996) and Flexas *et al.* (2007b). α values obtained were 0.94, 0.93 and 0.91 for leaves of N, SP and CL treatments, respectively.

Estimations of g_m were performed by the method by Harley *et al.* (1992):

$$g_m = A_N/(C_i - (\Gamma* \cdot (J_{flu} + 8 \cdot (A_N + R_l))/(J_{flu} - 4 \cdot (A_N + R_l))))$$

where A_N and C_i were taken from gas-exchange measurements at saturating light and R_l was estimated using the Laisk (1977) method. Only g_m data with dC_c/dA_N values between 10 and 50, which are reliable according to Harley *et al.* (1992), were used for analyses. Briefly, the Laisk method consisted in measuring A_N-C_i curves at three different PPFDs (50, 200, and 500 μmol m^{-2} sec^{-1}) with six different CO_2 concentrations ranging from 300 to 50 μmol CO_2 mol^{-1} air at each light intensity. A 2 × 3 cm LED chamber (LI-6400-02B) was used to measure A_N-C_i curves. The intersection point of the three A_N-C_i curves was used to determine R_l (y-axis). Although Laisk's method also can be used to estimate Γ*, it was decided to use the value at 25°C proposed for this parameter by Bernacchi *et al.* (2002) for this same species.

Finally, to estimate g_m and the photosynthetic capacity of the leaves (V_{cmax} and J_{max}) we used the curve fitting method proposed by Ethier and Livingston (2004). Six A_N-C_i response curves per treatment and date were performed in each treatment to determine the photosynthetic capacity of the leaves. After inducing steady-state photosynthesis (20–30 min of equilibrium time), the photosynthesis response to varying substomatal CO_2 concentration (C_i) was measured. C_a was lowered stepwise from 360 to 50 μmol mol^{-1} and then returned to 360 μmol mol^{-1} to re-establish the initial steady-state value of photosynthesis. C_a was then increased stepwise from 360 to 2000 μmol mol^{-1}. Gas-exchange measurements were determined at each step after maintaining the leaf for at least 5 min at the new C_a. Each A_N-C_i curve consisted of 12–13 measurements. CO_2 leakage into and out of the empty cuvette was determined at each cuvette CO_2 value and used to correct measured leaf fluxes following the method described by Flexas *et al.* (2007a). Maximum rate of RuBP carboxylation (V_{cmax}), maximum rate of electron transport (J_{max}) and g_m were determined by the fitting curve method described by Ethier and Livingston (2004). RI obtained in the analysis of Laisk curves was used.

Leaf anatomical parameters

To measure leaf thickness, histological preparations of tobacco leaves were done as previously described in Scafaro *et al.* (2011). Analyses of abaxial leaf cells were performed on epidermal impressions and epidermal peels. Epidermal impressions were obtained as previously described in Franco-Navarro *et al.* (2016) and analysed as reported in Gitz and Baker (2009).

To study the anatomical and subcellular properties of mesophyll cells, histological preparations of leaf transversal sections were performed. Tobacco leaves were sectioned by hand to obtain fragments of around 1–2 mm^2. These sections were fixed for 3 h at 4°C in 4% (v/v) glutaraldehyde in 0.1 M sodium cacodylate buffer (pH 7.4) and washed in the same buffer. Subsequently, leaf sections were post fixed for 2 h at 4°C in 1% (w/v) osmium tetroxide in 0.1 M sodium cacodylate buffer (pH 7.4) and washed in the same buffer. After fixation, fragments were dehydrated through graded alcohols and embedded in Epon resin (Epoxy Embedding Medium, Sigma). Semi-thin sections of 1–1.5 μm were stained with a 1% aqueous solution of toluidine blue for 1 min, rinsed with water, air-dried and mounted. Examination of epidermal peels and epidermal impressions as well as histological preparations were performed on Zeiss Axioskop and Olympus BX61 microscopes, respectively, and analysed by the Zeiss AxioVision software (following the manufacturer's specifications, https://www.zeiss.com/). Cell density and cell size were calculated as previously reported (Franco-Navarro *et al.*, 2016) using the Counterall® software (www.counterall.com; Bioscripts.net-IRNAS-CSIC) and the outline tool of the AxioVision Software, respectively. Epidermal cells density (ED) and Stomatal cells density (D) are defined by the total number of cells per leaf area (given in mm^2). The stomatal area (SA) was calculated as previously reported (Pompelli *et al.*, 2010):

$$\mathrm{SA} = \pi \times (\mathrm{SW}/2) \times (\mathrm{SL}/2)$$

where SW and SL are stomatal width and length.

Stomatal index (SI) is defined as the percentage number of stomata as compared to all the epidermal cells (including stomata) in a unit area of leaf (Salisbury, 1928):

$$\mathrm{SI}(\%) = (100 \cdot \mathrm{D})/(\mathrm{D} + \mathrm{ED})$$

Modelling of the maximum stomatal conductance ($g_{w,max}$) was calculated according to Franks *et al.* (2009). This equation is composed of: the diffusivity of water in air (d; 0.0000282 m^2 sec^{-1}); the mean maximum stomatal pore area (a_{max}; m^2) in a fraction (α; m^2) of stomatal cell size (S); the molar volume of air (v; 0.024465 m^3 mol^{-1}); and the stomatal density (D):

$$g_{w,max} = \frac{d\alpha D\sqrt{2S}}{v(0.5 + 0.627)\sqrt{\alpha}},$$

where

$$\alpha = (a_{max})/(S, \text{Stomatal cell size});$$

$$a_{max} = \pi \cdot (\text{stomatal pore length}/2)^2$$

Following the methodology described in Evans *et al.* (1994), different anatomical parameters of the mesophyll architecture were measured in histological preparations: palisade layer width, spongy layer width, mesophyll width without epidermal layer, leaf cross-section width, length and width of palisade cells, length and width of spongy cells. The surface area of mesophyll cells exposed to the intercellular airspaces (S_{mes}) was calculated using the curvature correction factor 'F' to convert cross-section length to surface area, assuming that mesophyll cells are spheroids with different width to height ratios (Thain, 1983):

$$S_{mes} = (L_{mes} \cdot F)/S_w$$

where L_{mes} is the length of mesophyll cells exposed to intercellular airspace, and S_w is the width of the cross-section.

The surface area of chloroplasts exposed to the intercellular airspace (S_c, $m^2\ m^{-2}$) was calculated according to the equation:

$$S_c = L_c/(L_{mes} \cdot S_{mes})$$

where L_c is the length of chloroplasts exposed to the intercellular airspaces.

Mesophyll and chloroplast surface area exposed to intercellular air spaces per leaf area were calculated separately for spongy and palisade tissues as described by Evans *et al.* (1994) and Syvertsen *et al.* (1995). Proportion of chloroplast covering the mesophyll cell surface was calculated from the ratio:

$$S_c/S_{mes}$$

Analysis of partitioning changes in photosynthesis rate

The difference in A_N among the three treatments result from the variation of the underlying variables directly related to CO_2 uptake and fixation: g_s, g_m and V_{cmax} (or J_{max}). The first two are involved in the chloroplasts CO_2 availability and are known as diffusional contributions (ρ_{diff}) to this change in A_N. The last two represent the contribution of the biochemical variables (ρ_{bio}) to this change in A_N. To partition the observed changes into contributions from these underlying variables, we used the contribution analysis proposed by Buckley and Diaz-Espejo (2015). This approach also allows accounting for contributions due to the RuBP regeneration region (represented by J_{max}), which was not considered in previous methods (Grassi and Magnani, 2005).

Starch determination

Starch was extracted from frozen leaves in ethanol 96%, following the method of Irigoyen *et al.* (1992). Later, the dried residue of the extraction was incubated in buffer acetate (4.5 mM), α-glucoamylase (0.5%, w/v) and water, for 48 h at 37°C. Starch concentration was analysed with anthrone reagent (Sigma-Aldrich) at an absorbance of 650 nm against a standard curve of sucrose, and was expressed as milligrams per gram of DW.

Statistical analysis

Statistical analysis was performed using the STATGRAPHICS Centurion XVI software (http://www.statgraphics.com; StatPoint Technologies, Warrenton, VA). Shapiro–Wilk (W) test was used to verify the normality of the data sets. One-way analysis of variance (ANOVA) and multivariate analysis of variance (MANOVA) tests were performed to determine significant differences between groups of samples, and levels of significance were described by asterisks: $P \leq 0.05$ (*); $P \leq 0.01$ (**); $P \leq 0.001$ (***). No significant (NS) differences were indicated when $P > 0.05$. Multiple comparisons of means were determined by the Tukey's Honest Significant Difference (HSD) and Multiple Range Test (MRT) statistical tests included in the mentioned software. Correlation between g_m estimations by Ethier and Harley was calculated through the Pearson's Product-Moment Correlation Coefficient (R^2). Values represent mean of at least five tobacco plants in each treatment, which were reproducible in at least two independent experiments.

ACKNOWLEDGEMENTS

This work was supported by the Spanish Ministry of Science Innovation and Universities-FEDER grants AGL2015-71386-R and RTI2018-094460-B-I00 and by the Spanish National Research Council grants CSIC-201540E108 and CSIC-201740E084. Help, expertise and technical assistance of F. J. Durán, C. Rivero and P. Benítez-Pulido are gratefully acknowledged.

CONFLICT OF INTEREST

The authors have no conflicts of interest to declare.

AUTHOR CONTRIBUTIONS

JDF-N and MAR conceived and performed the experiments, analysed the data, participated in the writing of the article as well as in the design of the research plans; PC-F participated in some experiments; RA and PC contributed to the microscopy assays; AD-E participated in conception of research plans, in the supervision of the experiments, and writing of the article; JMC-F conceived research plans, got the funds to finance the project, supervised the experiments, and wrote the article.

SUPPORTING INFORMATION

Additional Supporting Information may be found in the online version of this article.

Figure S1. Effect of Cl^- nutrition on plant and leaf growth.

Figure S2. Effect of Cl^- nutrition on water balance parameters.

Figure S3. Effect of different nutritional supplements on stomatal aperture.

Figure S4. Photomicrographs of leaves from plants grown with a mixture of sulphate + phosphate salts (SP); 5 mM nitrate salts (N) or 5 mM chloride salts (CL).

Figure S5. Correlation of the g_m estimation methods Ethier vs. Harley.

Table S1. Relation of nutritional treatments.

REFERENCES

Abbate, P.E., Dardanelli, J.L., Cantarero, M.G., Maturano, M., Melchiori, R.J.M. and Suero, E.E. (2004) Climatic and water availability effects on water-use efficiency in wheat. *Crop Sci.* **44**, 474–483. https://doi.org/10.2135/cropsci2004.4740

Allen, G.J., Kuchitsu, K., Chu, S.P., Murata, Y. and Schroeder, J.I. (1999) Arabidopsis *abi1-1* and *abi2-1* phosphatase mutations reduce abscisic acid-induced cytoplasmic calcium rises in guard cells. *Plant Cell*, **11**, 1785–1798. https://doi.org/10.2307/3871054

Bernacchi, C.J., Portis, A.R., Nakano, H., von Caemmerer, S. and Long, S.P. (2002) Temperature response of mesophyll conductance. Implications for the determination of Rubisco enzyme kinetics and for limitations to photosynthesis in vivo. *Plant Physiol.* **130**, 1992–1998. https://doi.org/10.1104/pp.008250

Bose, J., Munns, R., Shabala, S., Gilliham, M., Pogson, B. and Tyerman, S.D. (2017) Chloroplast function and ion regulation in plants growing on

saline soils: lessons from halophytes. *J. Exp. Bot.* **68**, 3129–3143. https://doi.org/10.1093/jxb/erx142

Boyer, J.S. (1996) Advances in drought tolerance in plants. *Adv. Agron.* **56**, 187–218. https://doi.org/10.1016/s0065-2113(08)60182-0

Buckley, T.N. and Diaz-Espejo, A. (2015) Partitioning changes in photosynthetic rate into contributions from different variables. *Plant Cell Environ.* **38**, 1200–1211. https://doi.org/10.1111/pce.12459

Carriqui, M., Douthe, C., Molins, A. and Flexas, J. (2019) Leaf anatomy does not explain apparent short-term responses of mesophyll conductance to light and CO2 in tobacco. *Physiol. Plant.* **165**, 604–618. https://doi.org/10.1111/ppl.12755

Cramer, M.D., Hawkins, H.-J. and Verboom, G.A. (2009) The importance of nutritional regulation of plant water flux. *Oecologia*, **161**, 15–24. https://doi.org/10.1007/s00442-009-1364-3

Cubero-Font, P., Maierhofer, T., Jaslan, J. *et al.* (2016) Silent S-type anion channel subunit SLAH1 gates SLAH3 open for chloride root-to-shoot translocation. *Curr. Biol.* **26**, 2213–2220. https://doi.org/10.1016/j.cub.2016.06.045

Dean, C. and Leech, R.M. (1982) Genome expression during normal leaf development. 1. Cellular and chloroplast numbers and DNA, RNA, and protein-levels in tissues of different ages within a 7-day-old wheat leaf. *Plant Physiol.* **69**, 904–910. https://doi.org/10.1104/pp.69.4.904

Duan, Z., Kong, F., Zhang, L., Li, W., Zhang, J. and Peng, L. (2016) A bestrophin-like protein modulates the proton motive force across the thylakoid membrane in Arabidopsis. *J. Integr. Plant Biol.* **58**, 848–858. https://doi.org/10.1111/jipb.12475

Enz, C., Steinkamp, T. and Wagner, R. (1993) Ion channels in the thylakoid membrane (a patch-clamp study). *Biochim. Biophys. Acta*, **1143**, 67–76. https://doi.org/10.1016/0005-2728(93)90217-4

Ethier, G.J. and Livingston, N.J. (2004) On the need to incorporate sensitivity to CO_2 transfer conductance into the Farquhar-von Caemmerer-Berry leaf photosynthesis model. *Plant Cell Environ.* **27**, 137–153. https://doi.org/10.1111/j.1365-3040.2004.01140.x

Evans, J. and Loreto, F. (2006) Acquisition and diffusion of CO_2 in higher plant leaves. In *Advances in Photosynthesis and Respiration*, Vol 9 (Leegood, R.C., Sharkey, T.D. and von Caemmerer, S., eds). Dordrecht, The Netherlands: Kluwer Academic Publishers, pp. 321–351.

Evans, J.R., Caemmerer, S.V., Setchell, B.A. and Hudson, G.S. (1994) The relationship between CO_2 transfer conductance and leaf anatomy in transgenic tobacco with a reduced content of Rubisco. *Funct. Plant Biol.* **21**, 475–495. https://doi.org/10.1071/pp9940475

Farquhar, G.D., Caemmerer, S.V. and Berry, J.A. (1980) A biochemical-model of photosynthetic CO_2 assimilation in leaves of C-3 species. *Planta*, **149**, 78–90. https://doi.org/10.1007/bf00386231

Flexas, J. (2016) Genetic improvement of leaf photosynthesis and intrinsic water use efficiency in C-3 plants: why so much little success? *Plant Sci.* **251**, 155–161. https://doi.org/10.1016/j.plantsci.2016.05.002

Flexas, J., Ribas-Carbo, M., Hanson, D.T., Bota, J., Otto, B., Cifre, J., McDowell, N., Medrano, H. and Kaldenhoff, R. (2006) Tobacco aquaporin NtAQP1 is involved in mesophyll conductance to CO_2 in vivo. *Plant J.* **48**, 427–439. https://doi.org/10.1111/j.1365-313x

Flexas, J., Diaz-Espejo, A., Berry, J.A., Galmés, J., Cifre, J., Kaldenhoff, R., Medrano, H. and Ribas-Carbo, M. (2007a) Analysis of leakage in IRGA's leaf chambers of open gas exchange systems: quantification and its effects in photosynthesis parameterization. *J. Exp. Bot.* **58**, 1533–1543. https://doi.org/10.1093/jxb/erm027

Flexas, J., Diaz-Espejo, A., Galmés, J., Kaldenhoff, R., Medrano, H. and Ribas-Carbo, M. (2007b) Rapid variations of mesophyll conductance in response to changes in CO_2 concentration around leaves. *Plant Cell Environ.* **30**, 1284–1298. https://doi.org/10.1111/j.1365-3040.2007.01700.x

Flexas, J., Ribas-Carbo, M., Diaz-Espejo, A., Galmés, J. and Medrano, H. (2008) Mesophyll conductance to CO_2: current knowledge and future prospects. *Plant Cell Environ.* **31**, 602–621. https://doi.org/10.1111/j.1365-3040.2007.01757.x

Flexas, J., Barbour, M.M., Brendel, O. *et al.* (2012) Mesophyll diffusion conductance to CO_2: an unappreciated central player in photosynthesis. *Plant Sci.* **193**, 70–84. https://doi.org/10.1016/j.plantsci.2012.05.009

Flexas, J., Niinemets, U., Galle, A. *et al.* (2013) Diffusional conductances to CO_2 as a target for increasing photosynthesis and photosynthetic water-use efficiency. *Photosynth. Res.* **117**, 45–59. https://doi.org/10.1007/s11120-013-9844-z

Flexas, J., Diaz-Espejo, A., Conesa, M.A. *et al.* (2016) Mesophyll conductance to CO_2 and Rubisco as targets for improving intrinsic water use efficiency in C-3 plants. *Plant Cell Environ.* **39**, 965–982. https://doi.org/10.1111/pce.12622

Flowers, T.J. (1988) Chloride as a nutrient and as an osmoticum. In *Advances in Plant Nutrition*, Vol. 3 (Tinker, B. and Läuchli, A., eds). New York: Praeger, pp. 55–78.

Franco-Navarro, J.D., Brumos, J., Rosales, M.A., Cubero-Font, P., Talon, M. and Colmenero-Flores, J.M. (2016) Chloride regulates leaf cell size and water relations in tobacco plants. *J. Exp. Bot.* **67**, 873–891. https://doi.org/10.1093/jxb/erv502

Franks, P.J., Drake, P.L. and Beerling, D.J. (2009) Plasticity in maximum stomatal conductance constrained by negative correlation between stomatal size and density: an analysis using *Eucalyptus globulus*. *Plant Cell Environ.* **32**, 1737–1748. https://doi.org/10.1111/j.1365-3040.2009.002031.x

Gago, J., Douthe, C., Florez-Sarasa, I., Escalona, J.M., Galmés, J., Fernie, A.R., Flexas, J. and Medrano, H. (2014) Opportunities for improving leaf water use efficiency under climate change conditions. *Plant Sci.* **226**, 108–119. https://doi.org/10.1016/j.plantsci.2014.04.007

Galmés, J., Ochogavia, J.M., Gago, J., Roldan, E.J., Cifre, J. and Conesa, M.A. (2013) Leaf responses to drought stress in Mediterranean accessions of Solanum lycopersicum: anatomical adaptations in relation to gas exchange parameters. *Plant Cell Environ.* **36**, 920–935. https://doi.org/10.1111/pce.12022

Geiger, D., Maierhofer, T., Al-Rasheid, K.A.S. *et al.* (2011) Stomatal closure by fast abscisic acid signaling is mediated by the guard cell anion channel SLAH3 and the receptor RCAR1. *Sci. Signal.* **4**, ra32. https://doi.org/10.1126/scisignal.2001346

Geilfus, C.M. (2018) Chloride: from nutrient to toxicant. *Plant Cell Physiol.* **59**, 877–886. https://doi.org/10.1093/pcp/pcy071

Genty, B., Briantais, J.M. and Baker, N.R. (1989) The relationship between the quantum yield of photosynthetic electron-transport and quenching of chlorophyll fluorescence. *Biochim. Biophys. Acta*, **990**, 87–92. https://doi.org/10.1016/s0304-4165(89)80016-9

Gilbert, N. (2012) Water under pressure. *Nature*, **483**, 256–257. https://doi.org/10.1038/483256a

Gitz, D.C. and Baker, J.T. (2009) Methods for creating stomatal impressions directly onto archivable slides. *Agron. J.* **101**, 232–236. https://doi.org/10.2134/agronj2008.0143n

Grassi, G. and Magnani, F. (2005) Stomatal, mesophyll conductance and biochemical limitations to photosynthesis as affected by drought and leaf ontogeny in ash and oak trees. *Plant Cell Environ.* **28**, 834–849. https://doi.org/10.1111/j.1365-3040.2005.01333.x

Gregory, P.J. (2004) Agronomic approaches to increasing water use efficiency. In *Water Use Efficiency in Plant Biology* (Bacon, M.A., ed). Oxford, UK: Blackwell Publishing Ltd, pp. 142–167.

Gu, L. and Sun, Y. (2014) Artefactual responses of mesophyll conductance to CO_2 and irradiance estimated with the variable J and online isotope discrimination methods. *Plant Cell Environ.* **37**, 1231–1249. https://doi.org/10.1111/pce.12232

Harley, P.C., Loreto, F., Dimarco, G. and Sharkey, T.D. (1992) Theoretical considerations when estimating the mesophyll conductance to CO_2 flux by analysis of the response of photosynthesis to CO_2. *Plant Physiol.* **98**, 1429–1436. https://doi.org/10.1104/pp.98.4.1429

Hassiotou, F., Ludwig, M., Renton, M., Veneklaas, E.J. and Evans, J.R. (2009) Influence of leaf dry mass per area, CO_2, and irradiance on mesophyll conductance in sclerophylls. *J. Exp. Bot.* **60**, 2303–2314. https://doi.org/10.1093/jxb/erp021

Hawkesford, M., Horst, W., Kichey, T., Lambers, H., Schjoerring, J., Skrumsager-Moller, I. and White, P.J. (2012) Functions of macronutrients. In *Marschner's Mineral Nutrition of Higher Plants* (Marschner P., ed). San Diego, USA: Academic Press, pp. 135–190.

He, J.-M., Ma, X.-G., Zhang, Y., Sun, T.-F., Xu, F.-F., Chen, Y.-P., Liu, X. and Yue, M. (2013) Role and interrelationship of G alpha protein, hydrogen peroxide, and nitric oxide in ultraviolet B-induced stomatal closure in Arabidopsis leaves. *Plant Physiol.* **161**, 1570–1583. https://doi.org/10.1104/pp.112.211623

Heber, U. and Heldt, H.W. (1981) The chloroplast envelope: structure, function, and role in leaf metabolism. *Annu. Rev. Plant Biol.* **32**, 139–168. https://doi.org/10.1146/annurev.pp.32.060181.001035

Henriques, F.S. (2004) Reduction in chloroplast number accounts for the decrease in the photosynthetic capacity of Mn-deficient pecan leaves. *Plant Sci.* **166**, 1051–1055. https://doi.org/10.1016/j.plantsci.2003.12.022

Herdean, A., Nziengui, H., Zsiros, O., Solymosi, K., Garab, G., Lundin, B. and Spetea, C. (2016a) The Arabidopsis thylakoid chloride channel AtCLCe functions in chloride homeostasis and regulation of photosynthetic electron transport. *Front. Plant Sci.* **7**, 115. https://doi.org/10.3389/fpls.2016.00115

Herdean, A., Teardo, E., Nilsson, A.K. *et al.* (2016b) A voltage-dependent chloride channel fine-tunes photosynthesis in plants. *Nat. Commun.* **7**, 11654. https://doi.org/10.1038/ncomms11654

Hind, G., Nakatani, H.Y. and Izawa, S. (1974) Light-dependent redistribution of ions in suspensions of chloroplast thylakoid membranes. *Proc. Natl Acad. Sci. USA*, **71**, 1484–1488. https://doi.org/10.1073/pnas.71.4.1484

Irigoyen, J.J., Emerich, D.W. and Sánchez-Díaz, M. (1992) Water-stress induced changes in concentrations of proline and total soluble sugars in nodulated alfalfa (*Medicago sativa*) plants. *Physiol. Plant.* **84**, 55–60. https://doi.org/10.1111/j.1399-3054.1992.tb08764.x.

Jin, B., Wang, L., Wang, J., Jiang, K.Z., Wang, Y., Jiang, X.X., Ni, C.Y., Wang, Y.L. and Teng, N.J. (2011) The effect of experimental warming on leaf functional traits, leaf structure and leaf biochemistry in *Arabidopsis thaliana*. *BMC Plant Biol.* **11**, 35. https://doi.org/10.1186/1471-2229-11-35

Johnson, C.M., Stout, P.R., Broyer, T.C. and Carlton, A.B. (1957) Comparative chlorine requirements of different plant species. *Plant Soil*, **8**, 337–353. https://doi.org/10.1007/bf01666323

Kawakami, K., Umena, Y., Kamiya, N. and Shen, J.-R. (2009) Location of chloride and its possible functions in oxygen-evolving photosystem II revealed by X-ray crystallography. *Proc. Natl Acad. Sci. USA*, **106**, 8567–8572. https://doi.org/10.1073/pnas.0812797106

Kirchhoff, H. (2014) Structural changes of the thylakoid membrane network induced by high light stress in plant chloroplasts. *Philos. Trans. R. Soc. Lond. B Biol. Sci.*, **369**, 20130225. https://doi.org/10.1098/rstb.2013.0225

Laisk, A.K. (1977) *Kinetics of Photosynthesis and Photorespiration in C3 Plants*. Moscow: Nauka Publishing.

Lake, J.A., Quick, W.P., Beerling, D.J. and Woodward, F.I. (2001) Plant development – signals from mature to new leaves. *Nature*, **411**, 154–154. https://doi.org/10.1038/35075660

Li, Y., Gao, Y., Xu, X., Shen, Q. and Guo, S. (2009) Light-saturated photosynthetic rate in high-nitrogen rice (*Oryza sativa* L.) leaves is related to chloroplastic CO_2 concentration. *J. Exp. Bot.* **60**, 2351–2360. https://doi.org/10.1093/jxb/erp127

Li, B., Tester, M. and Gilliham, M. (2017) Chloride on the move. *Trends Plant Sci.* **22**, 236–248. https://doi.org/10.1016/j.tplants.2016.12.004

Linderson, M.L., Mikkelsen, T.N., Ibrom, A., Lindroth, A., Ro-Poulsen, H. and Pilegaard, K. (2012) Up-scaling of water use efficiency from leaf to canopy as based on leaf gas exchange relationships and the modeled in-canopy light distribution. *Agric. For. Meteorol.* **152**, 201–211. https://doi.org/10.1016/j.agrformet.2011.09.019

Liu, H.C., Wang, X.X., Ren, K.X., Li, K., Wei, M.M., Wang, W.J. and Sheng, X.Y. (2017) Light deprivation-induced inhibition of chloroplast biogenesis does not arrest embryo morphogenesis but strongly reduces the accumulation of storage reserves during embryo maturation in Arabidopsis. *Front. Plant Sci.* **8**, 14. https://doi.org/10.3389/fpls.2017.01287

Long, S.P., Zhu, X.G., Naidu, S.L. and Ort, D.R. (2006) Can improvement in photosynthesis increase crop yields? *Plant Cell Environ.* **29**, 315–330. https://doi.org/10.1111/j.1365-3040.2005.01493.x

Losch, R., Jensen, C.R. and Andersen, M.N. (1992) Diurnal courses and factorial dependencies of leaf conductance and transpiration of differently potassium fertilized and watered field-grown barley plants. *Plant Soil*, **140**, 205–224. https://doi.org/10.1007/bf00010598

Lu, Z., Lu, J., Pan, Y., Lu, P., Li, X., Cong, R. and Ren, T. (2016) Anatomical variation of mesophyll conductance under potassium deficiency has a vital role in determining leaf photosynthesis. *Plant Cell Environ.* **39**, 2428–2439. https://doi.org/10.1111/pce.12795

Marschner, H. (2011) *Mineral Nutrition of Higher Plants*. London, UK: Academic Press.

McAdam, S.A.M. and Brodribb, T.J. (2016) Linking turgor with ABA biosynthesis: implications for stomatal responses to vapor pressure deficit across land plants. *Plant Physiol.* **171**, 2008–2016. https://doi.org/10.1104/pp.16.00380

McAdam, S.A.M. and Brodribb, T.J. (2018) Mesophyll cells are the main site of abscisic acid biosynthesis in water-stressed leaves. *Plant Physiol.* **177**, 911–917. https://doi.org/10.1104/pp.17.01829

Meidner, H. and Willmer, C.M. (1993) Circadian-rhythm of stomatal movements in epidermal strips. *J. Exp. Bot.* **44**, 1649–1652. https://doi.org/10.1093/jxb/44.11.1649

Meyer, S., Mumm, P., Imes, D., Endler, A., Weder, B., Al-Rasheid, K.A.S., Geiger, D., Marten, I., Martinoia, E. and Hedrich, R. (2010) AtALMT12 represents an R-type anion channel required for stomatal movement in Arabidopsis guard cells. *Plant J.* **63**, 1054–1062. https://doi.org/10.1111/j.1365-313x.2010.04302.x

Momayyezi, M. and Guy, R.D. (2017) Substantial role for carbonic anhydrase in latitudinal variation in mesophyll conductance of *Populus trichocarpa* Torr. & Gray. *Plant Cell Environ.* **40**, 138–149. https://doi.org/10.1111/pce.12851

Morison, J.I.L., Baker, N.R., Mullineaux, P.M. and Davies, W.J. (2008) Improving water use in crop production. *Philos. Trans. R. Soc. Lond. B Biol. Sci.* **363**, 639–658. https://doi.org/10.1098/rstb.2007.2175

Muir, C.D., Hangarter, R.P., Moyle, L.C. and Davis, P.A. (2014) Morphological and anatomical determinants of mesophyll conductance in wild relatives of tomato (Solanum sect. Lycopersicon, sect. Lycopersicoides; Solanaceae). *Plant Cell Environ.* **37**, 1415–1426. https://doi.org/10.1111/pce.12245

Negi, J., Matsuda, O., Nagasawa, T., Oba, Y., Takahashi, H., Kawai-Yamada, M., Uchimiya, H., Hashimoto, M. and Iba, K. (2008) CO_2 regulator SLAC1 and its homologues are essential for anion homeostasis in plant cells. *Nature*, **452**, 483–U13. https://doi.org/10.1038/nature06720

Oddo, E., Inzerillo, S., La Bella, F., Grisafi, F., Salleo, S. and Nardini, A. (2011) Short-term effects of potassium fertilization on the hydraulic conductance of *Laurus nobilis* L. *Tree Physiol.* **31**, 131–138. https://doi.org/10.1093/treephys/tpq115

Ort, D.R., Merchant, S.S., Alric, J. *et al.* (2015) Redesigning photosynthesis to sustainably meet global food and bioenergy demand. *Proc. Natl Acad. Sci. USA*, **112**, 8529–8536. https://doi.org/10.1073/pnas.1424031112

Paoleti, E. and Gellini, R. (1993) Stomatal density variation in beech and holm oak leaves collected over the last 200 years. *Acta Oecologica*, **14**, 173–178.

Parry, M.A.J., Flexas, J. and Medrano, H. (2005) Prospects for crop production under drought: research priorities and future directions. *Ann. Appl. Biol.* **147**, 211–226. https://doi.org/10.1111/j.1744-7348.2005.00032.x

Pompelli, M.F., Martins, S.C.V., Celin, E.F., Ventrella, M.C. and DaMatta, F.M. (2010) What is the influence of ordinary epidermal cells and stomata on the leaf plasticity of coffee plants grown under full-sun and shady conditions? *Braz. J. Biol.* **70**, 1083–1088. https://doi.org/10.1590/s1519-69842010000500025

Pyke, K.A. (2010) Plastid division. *Aob Plants*, plq016. https://doi.org/10.1093/aobpla/plq016

Pyke, K.A. and Leech, R.M. (1987) The control of chloroplast number in wheat mesophyll-cells. *Planta*, **170**, 416–420. https://doi.org/10.1007/bf00395035

Pyke, K.A. and Leech, R.M. (1992) Chloroplast division and expansion is radically altered by nuclear mutations in *Arabidopsis thaliana*. *Plant Physiol.* **99**, 1005–1008. https://doi.org/10.1104/pp.99.3.1005

Raven, J.A. (2017) Chloride: essential micronutrient and multifunctional beneficial ion. *J. Exp. Bot.* **68**, 359–367. https://doi.org/10.1093/jxb/erw421

Rios, J.J., Blasco, B., Cervilla, L.M., Rubio-Wilhelmi, M.M., Rosales, M.A., Sanchez-Rodriguez, E., Romero, L. and Ruiz, J.M. (2010) Nitrogen-use efficiency in relation to different forms and application rates of se in lettuce plants. *J. Plant Growth Regul.* **29**, 164–170. https://doi.org/10.1007/s00344-009-9130-7

Sack, L., John, G.P. and Buckley, T.N. (2018) ABA accumulation in dehydrating leaves is associated with decline in cell volume, not turgor pressure. *Plant Physiol.* **176**, 489–495. https://doi.org/10.1104/pp.17.01097

Salisbury, E.J. (1928) On the causes and ecological significance of stomatal frequency, with special reference to the woodland flora. *Phil. Trans. R. Soc. Lond. B*, **216**, 1–65. https://doi.org/10.1098/rstb.1928.0001

Scafaro, A.P., Von Caemmerer, S., Evans, J.R. and Atwell, B.J. (2011) Temperature response of mesophyll conductance in cultivated and wild Oryza species with contrasting mesophyll cell wall thickness. *Plant Cell Environ.* **34**, 1999–2008. https://doi.org/10.1111/j.1365-3040.2011.02398.x

Schultz, H.R. (1996) Leaf absorptance of visible radiation in *Vitis vinifera* L.: estimates of age and shade effects with a simple field method. *Sci. Hort.* **66**, 93–102. https://doi.org/10.1016/0304-4238(96)00876-x

Schulze, E.D., Kelliher, F.M., Korner, C., Lloyd, J. and Leuning, R. (1994) Relationships among maximum stomatal conductance, ecosystem surface conductance, carbon assimilation rate, and plant nitrogen nutrition – a global ecology scaling exercise. *Annu. Rev. Ecol. Evol.* **25**, 629–662. https://doi.org/10.1146/annurev.es.25.110194.003213

Syvertsen, J.P., Lloyd, J., McConchie, C., Kriedemann, P.E. and Farquhar, G.D. (1995) On the relationship between leaf anatomy and CO_2 diffusion through the mesophyll of hypostomatous leaves. *Plant Cell Environ.* **18**, 149–157. https://doi.org/10.1111/j.1365-3040.1995.tb00348.x

Szabo, I. and Spetea, C. (2017) Impact of the ion transportome of chloroplasts on the optimization of photosynthesis. *J. Exp. Bot.* **68**, 3115–3128. https://doi.org/10.1093/jxb/erx063

Teng, N., Wang, J., Chen, T., Wu, X., Wang, Y. and Lin, J. (2006) Elevated CO_2 induces physiological, biochemical and structural changes in leaves of *Arabidopsis thaliana*. *New Phytol.* **172**, 92–103. https://doi.org/10.1111/j.1469-8137.2006.01818.x

Terashima, I., Hanba, Y.T., Tazoe, Y., Vyas, P. and Yano, S. (2006) Irradiance and phenotype: comparative eco-development of sun and shade leaves in relation to photosynthetic CO_2 diffusion. *J. Exp. Bot.* **57**, 343–354. https://doi.org/10.1093/jxb/erj014

Terashima, I., Hanba, Y.T., Tholen, D. and Niinemets, U. (2011) Leaf functional anatomy in relation to photosynthesis. *Plant Physiol.* **155**, 108–116. https://doi.org/10.1104/pp.110.165472

Terry, N. (1977) Photosynthesis, growth, and role of chloride. *Plant Physiol.* **60**, 69–75. https://doi.org/10.1104/pp.60.1.69

Thain, J.F. (1983) Curvature correction factors in the measurement of cell-surface areas in plant-tissues. *J. Exp. Bot.* **34**, 87–94. https://doi.org/10.1093/jxb/34.1.87

Tholen, D. and Zhu, X.-G. (2011) The mechanistic basis of internal conductance: a theoretical analysis of mesophyll cell photosynthesis and CO_2 diffusion. *Plant Physiol.* **156**, 90–105. https://doi.org/10.1104/pp.111.172346

Ticha, I. (1982) Photosynthetic characteristics during ontogenesis of leaves.7. stomata density and sizes. *Photosynthetica*, **16**, 375–471.

Tomas, M., Flexas, J., Copolovici, L., Galmés, J., Hallik, L., Medrano, H., Ribas-Carbo, M., Tosens, T., Vislap, V. and Niinemets, U. (2013) Importance of leaf anatomy in determining mesophyll diffusion conductance to CO_2 across species: quantitative limitations and scaling up by models. *J. Exp. Bot.* **64**, 2269–2281. https://doi.org/10.1093/jxb/ert086

Tomas, M., Medrano, H., Escalona, J.M., Martorell, S., Pou, A., Ribas-Carbo, M. and Flexas, J. (2014) Variability of water use efficiency in grapevines. *Environ. Exp. Bot.* **103**, 148–157. https://doi.org/10.1016/j.envexpbot.2013.09.003

Tomeo, N.J. and Rosenthal, D.M. (2017) Variable mesophyll conductance among soybean cultivars sets a tradeoff between photosynthesis and water-use-efficiency. *Plant Physiol.* **174**, 241–257. https://doi.org/10.1104/pp.16.01940

Tosens, T., Niinemets, U., Vislap, V., Eichelmann, H. and Castro Diez, P. (2012) Developmental changes in mesophyll diffusion conductance and photosynthetic capacity under different light and water availabilities in Populus tremula: how structure constrains function. *Plant Cell Environ.* **35**, 839–856. https://doi.org/10.1111/j.1365-3040.2011.02457.x

Uehlein, N., Lovisolo, C., Siefritz, F. and Kaldenhoff, R. (2003) The tobacco aquaporin NtAQP1 is a membrane CO_2 pore with physiological functions. *Nature*, **425**, 734–737. https://doi.org/10.1038/nature02027

Vahisalu, T., Kollist, H., Wang, Y.-F. *et al.* (2008) SLAC1 is required for plant guard cell S-type anion channel function in stomatal signalling. *Nature*, **452**, 487–491. https://doi.org/10.1038/nature06608

Wang, M., Lee, J., Choi, B., Park, Y., Sim, H.-J., Kim, H. and Hwang, I. (2018) Physiological and molecular processes associated with long duration of ABA treatment. *Front. Plant Sci.* **9**, 176. https://doi.org/10.3389/fpls.2018.00176

Warren, C.R. (2008) Stand aside stomata, another actor deserves centre stage: the forgotten role of the internal conductance to CO(2) transfer. *J. Exp. Bot.* **59**, 1475–1487. https://doi.org/10.1093/jxb/erm245

Wege, S., Gilliham, M. and Henderson, S.W. (2017) Chloride: not simply a 'cheap osmoticum', but a beneficial plant macronutrient. *J. Exp. Bot.* **68**, 3057–3069. https://doi.org/10.1093/jxb/erx050

Weise, S.E., Carr, D.J., Bourke, A.M., Hanson, D.T., Swarthout, D. and Sharkey, T.D. (2015) The arc mutants of Arabidopsis with fewer large chloroplasts have a lower mesophyll conductance. *Photosynth. Res.* **124**, 117–126. https://doi.org/10.1007/s11120-015-0110-4

White, P.J. and Broadley, M.R. (2001) Chloride in soils and its uptake and movement within the plant: a review. *Ann. Bot.* **88**, 967–988. https://doi.org/10.1006/anbo.2001.1540

Wilkinson, S., Bacon, M.A. and Davies, W.J. (2007) Nitrate signalling to stomata and growing leaves: interactions with soil drying, ABA, and xylem sap pH in maize. *J. Exp. Bot.* **58**, 1705–1716. https://doi.org/10.1093/jxb/erm021

Willmer, C.M. and Fricker, M.D., editors (1996) Stomata. In *Topics in Plant Functional Biology*, Vol. **2**. The Netherlands: Springer, pp. 92–109. https://doi.org/10.1007/978-94-011-0579-8

Wright, I.J., Reich, P.B. and Westoby, M. (2003) Least-cost input mixtures of water and nitrogen for photosynthesis. *Am. Nat.* **161**, 98–111. https://doi.org/10.1086/344920

Xiao, Y. and Zhu, X.-G. (2017) Components of mesophyll resistance and their environmental responses: a theoretical modelling analysis. *Plant Cell Environ.* **40**, 2729–2742. https://doi.org/10.1111/pce.13040

Xiong, D.L., Huang, J.L., Peng, S.B. and Li, Y. (2017) A few enlarged chloroplasts are less efficient in photosynthesis than a large population of small chloroplasts in *Arabidopsis thaliana*. *Sci. Rep.* **7**, 12. https://doi.org/10.1038/s41598-017-06460-0

Xu, G.H., Magen, H., Tarchitzky, J. and Kafkafi, U. (2000) Advances in chloride nutrition of plants. In *Advances in Agronomy*, Vol. 68 (Sparks, D.L., ed). San Diego, USA: Elsevier Academic Press Inc, pp. 97–150.

Zhu, X.-G., Long, S.P. and Ort, D.R. (2010) Improving photosynthetic efficiency for greater yield. *Annu. Rev. Plant Biol.* **61**, 235–261. https://doi.org/10.1146/annurev-arplant-042809-112206

Zimmermann, D., Reuss, R., Westhoff, M., Gessner, P., Bauer, W., Bamberg, E., Bentrup, F.W. and Zimmermann, U. (2008) A novel, non-invasive, online-monitoring, versatile and easy plant-based probe for measuring leaf water status. *J. Exp. Bot.* **59**, 3157–3167. https://doi.org/10.1093/jxb/ern171

Zimmermann, U., Rüger, S., Shapira, O. *et al.* (2010) Effects of environmental parameters and irrigation on the turgor pressure of banana plants measured using the non-invasive, online monitoring leaf patch clamp pressure probe. *Plant Biol.* **12**, 424–436. https://doi.org/10.1111/j.1438-8677.2009.00235.x

